SIMULATING THE EFFECTS OF BARRIER ISLAND SCALE ON STORM SURGE ATTENUATION

by

SHEPPARD DANIEL MEDLIN

(Under the Direction of Matthew Vernon Bilskie)

ABSTRACT

Natural and Nature-Based Features (NNBF) are an increasingly attractive flood mitigation solution. Barrier islands (BI) are a type of NNBF but information is lacking on the spatial scales at which BI attenuate substantial levels of storm surge. This thesis fills that gap by quantifying scaling relationships between BI characteristics and their flood response for a variety of synthetic storms. Idealized models of coastal landscapes containing BI were generated from a compiled database of BI morphological data. These landscapes, along with synthetic storm surge forcings, were used as inputs to the ADvanced CIRCulation model (ADCIRC). BI morphological parameters were individually adjusted to determine their effect on storm surge inundation. BI reduce maximum water elevations by up to 61% depending on dune height, ratio of inlet width to island length, and storm duration. These results will encourage the use of BI as flood risk reduction infrastructure.

INDEX WORDS: Barrier Island, Natural and Nature-Based Features, Numerical Modeling, Coastal Flooding, ADCIRC

SIMULATING THE EFFECTS OF BARRIER ISLAND SCALE ON STORM SURGE ATTENUATION

by

SHEPPARD DANIEL MEDLIN

BS, North Carolina State University, 2019

A Thesis Submitted to the Graduate Faculty of The University of Georgia in Partial Fulfillment of the Requirements for the Degree

MASTER OF SCIENCE

ATHENS, GEORGIA

2022

SIMULATING THE EFFECTS OF BARRIER ISLAND SCALE ON STORM SURGE ATTENUATION

by

SHEPPARD MEDLIN

Major Professor: Matthew Vernon Bilskie
Committee: Brian Bledsoe
Brock Woodson

Electronic Version Approved:

Ron Walcott
Vice Provost for Graduate Education and Dean of the Graduate School
The University of Georgia
August 2022

To my family

ACKNOWLEDGEMENTS

The following work would not have been possible without the knowledge, guidance, and aid of both friends and colleagues. Most importantly, I'd like to express my deepest appreciation to Dr. Matthew Bilskie for taking me in as his first student at UGA. I am extremely grateful for his support and mentorship over the past two years. I'd also like to thank Dr. Brian Bledsoe and Dr. Brock Woodson for their valuable feedback while serving on my thesis committee.

I have been honored to watch the COAST Lab grow into the thriving community it is today. Few places are as welcoming and engaging as here. Special thanks to Dr. Felix Luis Santiago Collazo and Dr. Viyaktha Hithaishi Hewageegana for their first-class mentorship. I'd like to express my gratitude to Robert Fiegelist, Becca Stanley, Ada Chimzulukeme Agbogu, Caraline Miller, Oscar Villegas Gutierrez, Grant Bilderback and Nashid Mumtaz for their support and camaraderie.

I am extremely grateful to Dr. Julia Mulhern who provided much of the data that inspired this thesis. Many thanks to professional colleagues, Dr. Casey Dietrich and Johnathan Woodruff of NC State University; Dr. Amanda Tritinger, Dr. Candice Pearcy, and Dr. Margaret Owensby of the U.S. Army Corps of Engineers; and everybody on the N-EWN® Team who I do not have space to thank individually.

Words cannot express my gratitude for my parents and sister, whose unconditional love and support throughout my life has given me the confidence to try, and often fail at, accomplishing my goals. Lastly, I am extremely grateful for my partner, whose patience and love knows no bounds. I could not have undertaken this journey without all of you.

This work was supported by the U.S. Army Corps of Engineers Engineering With Nature® Initiative through Cooperative Ecosystem Studies Unit Agreement W912HZ2020031.

TABLE OF CONTENTS

Page

LIST OF TABLES

Page

LIST OF FIGURES

Page

CHAPTER 1 INTRODUCTION

Nearly 30% of the United States population lives in counties bordering a coastline. Of that group, 60.2 million people, or about 1 in 6 Americans, live along the Gulf of Mexico or the Atlantic Coast, the regions most susceptible to hurricanes and storm surge. Additionally, the Gulf Coast is one of the fastest-growing regions in the United States. Gulf coast counties grew by 26% from 2000-2016, compared with an average growth rate of 15.7% for the United States (Cohen, 2019). This means that an ever-increasing portion of the American population is exposed to hurricane-related hazards every year.

Hurricanes are both the costliest and the deadliest natural disasters on the planet. From 1980-2021 the total cost of damages from the largest hurricane events (more than $1 billion per event) totaled over $1.1 trillion in the United States alone (CPI adjusted to 2022). In the same timeframe, hurricanes also caused 6,708 deaths in the United States, the highest number of any category of natural weather events (NCEI, 2022). It is estimated that hurricane-induced flooding causes $20 billion in annual damage (Terry Dinan, 2019). It is of utmost importance that damages from hurricanes, particularly hurricane-induced flooding, be minimized to the greatest extent possible.

When discussing the impact of hurricanes and other natural disasters, the terms hazard, risk, vulnerability, and resilience are often used interchangeably, but they are not the same concept. Natural hazards are naturally occurring events that can cause harm to people. Examples of natural hazards include hurricanes and storm surge, among other natural phenomena. Vulnerability is generally considered to be “the propensity or predisposition to be adversely affected” and is a function of exposure, sensitivity, and adaptive capacity (IPCC, 2022). Risk

however, is the probability of damage or loss due to a hazardous event. This can include economic, social, human (death), and environmental losses. Risk can be quantified in several ways, but it is generally considered the product of hazard severity and a community's vulnerability to the hazard (Hernández et al., 2018). When people, communities, or infrastructure can resist a loss in function due to disturbances (natural hazards) or quickly return to their baseline condition after a disturbance has caused a loss in function, they are considered to have resilience (Rosati et al., 2015; Schultz, 2012). However, it could be argued that resilience would indicate a community's ability to bounce back to a less vulnerable state after a disturbance.

To reduce the risk associated with coastal flooding events, engineers, coastal planners, and community stakeholders have recently been turning towards Nature-Based Features (NBF) as they have potential to offer increased resilience and co-benefits when compared to traditional infrastructure. NBF are any infrastructure designed and built by humans that intentionally mimics nature in its form and/or function (Bridges et al., 2015). Examples of commonly implemented NBFs include living shorelines, constructed wetlands, constructed sand dunes, and beach nourishment projects. This topic will be covered in-depth in Chapter 2.2, but it is important to note that NBFs have several challenges to overcome before becoming as prevalent as conventional forms of infrastructure. More research needs to be conducted on several types of NBFs to understand their abilities and weaknesses, particularly when it comes to flood attenuation.

While nearly all existing BI are naturally occurring, there is a growing interest in restoring existing BI and constructing new BI to be used as flood mitigation infrastructure. However, the use of restored and constructed BI as NBF is hindered by the lack of research into the spatial

scales at which BI attenuate meaningful amounts of storm surge. This thesis addresses this gap in information by attempting to accomplish the following three research objectives:

1. Improve understanding of how BI attenuate storm surge, particularly how storm surge is affected by the physical scales at which BI occur;
2. Create new tools to aid engineers in restoring and designing BI for coastal flood protection; and
3. Increase available data on BI morphology to assist in future BI modeling efforts.

Three research questions guided these overarching research objectives.

1. Which variables are most relevant for reducing the depth and duration of storm surge flood events in terms of BI scale and configuration?
2. Between BI scale, BI configuration, and storm characteristics, which factor, or combination of factors has the most impact on the depth and duration of storm surge flooding?
3. Using what is learned from the preceding questions, can we identify BI configuration(s) that maximize flood protection?

The remainder of this thesis is laid out as follows. Chapter 2is a Literature Review covering the history of flood hazard mitigation infrastructure in the United States, the recent shift to NBF, and how hydrodynamic models have been used to predict NBF performance. Chapter 3 is a journal manuscript containing a further introduction, methods, results, and a preliminary discussion. Finally, Chapter 4 contains further discussion and conclusions

CHAPTER 2 LITERATURE REVIEW

This chapter presents a literature review on three main topics: 1) Conventional flood hazard reduction in the United States; 2) an introduction to NBF; and 3) using computational modeling to aid the development of NBF.

2.1 Conventional Flood Hazard Reduction in the U.S.

Controlling flood hazards is often the most direct route to flood risk reduction and is the default technique to mitigate flood risk in the United States. A flood hazard is a naturally occurring severe weather event that causes flooding. Some examples of flood hazards include storm surge, waves, and heavy rain events. Flood hazard reduction is generally accomplished through installing flood mitigation infrastructure and can take the form of either traditional, natural, or nature-based infrastructure. Such infrastructure helps reduce the severity of flooding by reducing maximum water levels and the duration of high water. Flood hazard reduction is often seen as having great value, especially in populated areas. It doubles as flood risk reduction in areas where flood hazards overlap with vulnerable manmade structures and systems.

Historically, flood hazard reduction and prevention in the United States was accomplished through engineered structures. Flood mitigation infrastructure was occasionally funded on a federal level starting with the Flood Control Act of 1917, which helped fund levees in the Mississippi and Sacramento River deltas (Arnold, 1988; Bergsma, 2018). This was followed by the Flood Control Act of 1928, which fully financed the construction of levees in Mississippi (Barry 1977). Between 1936 and 1948, no less than eight more Flood Control Acts were passed as part of Franklin D. Roosevelt's "New Deal." Among other things, these acts

permanently delegated the construction of flood mitigation infrastructure to the U.S. Army Corps of Engineers (USACE) (Bergsma 2019, Arnold 1988). The USACE methods of flood hazard reduction included the construction of dikes, levees, and other "conventional" infrastructure. These structures remained the status-quo and only federally funded option for reducing flood risk until the 1968 creation of the National Flood Insurance Program (NFIP). According to Bergsma, the NFIP is the United States' way of implementing a Flood Risk Management (FRM) policy alongside their flood hazard reduction goals. The goal of the NFIP is to discourage development in flood-prone regions to reduce the cost of flood reduction investments and the cost of necessary aid when those areas flood (Arnell, 1984). However, the U.S. Army Corps of Engineers still engages in many flood hazard mitigation projects (Wood et al., 2012).

In the context of this literature review, "conventional" infrastructure refers to the types of flood hazard mitigation infrastructure talked about thus far. This type of infrastructure is generally impervious, entirely human-engineered, and often made of concrete. Examples in the coastal environment include, dikes, levees, seawalls, breakwaters, jetties, and bulkheads (Bulleri & Chapman, 2010). Other names for conventional infrastructure include "traditional", "engineered", "built", or "hard" infrastructure. Much of the conventional infrastructure in the U.S., including flood reduction infrastructure, needs repair and reinvestment to prevent failure and continue to provide community benefits (ASCE, 2016).

As storms become more intense and sea levels continue to rise due to climate change, infrastructure resilience will become more important than ever. Hinkel et al. (2014) modeled the effects of population growth and sea level rise on the total number of people flooded and the total damages due to floods in 2100. Flood damages were found to amount to 0.3%-9.3% of global GDP without taking any adaptive flood management measures. However, an adaptive

management technique to reduce flood costs results in $12-$71 billion/year in investment and maintenance costs in dikes globally by 2100 (Hinkel et al., 2014).

While sea level rise may be one of the most significant impacts on our flood management infrastructure, other impacts may include increased intensity of hurricanes, especially in the North Atlantic (IPCC, 2021). Additionally, the IPCC noted that the pace of sea level rise appears to be increasing along with the rate of global warming. Flood mitigation infrastructure needs to be able to adapt to these changing conditions over the course of the 21st century to save lives and reduce economic damages. In other words, flood mitigation infrastructure needs to be resilient.

Many have already outlined the need for resilient infrastructure, however ideas on how resilient infrastructure should be implemented vary greatly (Chester et al., 2021; Gersonius et al., 2013; Hinkel et al., 2014; Kim et al., 2019; Liao, 2012; Rosati et al., 2015; Schultz, 2012). Gersonius et al. (2013) argued for adopting a Real in Options (RIO) analysis in the planning stages for our flood mitigation infrastructure to account for uncertainties around the future global climate. Other authors argued that we should move away from the current paradigm that infrastructure should be fail-safe and move to a paradigm where infrastructure is safe-to-fail. In this framework, infrastructure is designed, and policy is made, with the intent that the infrastructure may fail, and if it does, impacts in the form of economic damages and loss of life would be minimized. This contrasts with the current fail-safe paradigm, where infrastructure is designed not to fail. If failure happens, it is often catastrophic in nature (Kim et al. 2019). Others have recommended a full overhaul in our bureaucratic and educational systems that prioritize agility and information flow across disparate fields to effectively implement resilient infrastructure over time (Chester et al. 2021).

In the face of these changing demands on flood reduction infrastructure, some of the inherent limitations of conventional infrastructure design become evident. Most conventional flood mitigation infrastructure cannot adapt to changing environmental conditions without human intervention (Hinkel et al. 2014). In other words, conventional infrastructure is a static rather than a dynamic (or resilient) solution to flood risk reduction (Chester et al. 2021). This presents a challenge in a rapidly changing environment. Ideally, once the infrastructure is built, it will function properly for the duration of its design life. Similarly, conventional infrastructure is in a constant state of degradation once it has been built (Sutton-Grier et al., 2018). This can lead to ever-increasing maintenance and operating costs that may not have been accounted for in the original design. Conventional infrastructure is also inherently at odds with the environment as it removes natural landscapes and replaces them with rigid, impervious structures that often do not provide the same level of ecosystem services that that natural habitat provide (Bulleri & Chapman, 2010; Chester et al., 2021; Morris et al., 2018).

2.2 Introduction to NBF

Resulting from the shortcomings of traditional infrastructure, Natural and Nature-Based Features (NNBF) have been gaining popularity in recent years. NNBF is a blanket term referring to two different types of infrastructure, Nature-Based Features (NBF) and Natural Features (NF). NF, by definition, “are created and evolve over time through the actions of physical, biological, geologic, and chemical processes operating in nature”. Most BI, mangroves, salt marshes, and sand dunes are NF. Nature Based Features (NBF) differ from conventional infrastructure and NF in that they are designed and engineered by humans to mimic naturally occurring features to serve a specific purpose (Bridges et al., 2015). Examples of more common NBF include living shorelines, and beach nourishment projects. However, many types of NF can

be designed and built as NBF. Wetlands and sand dunes are occasionally constructed as a form of NBF and entire BI could be too. Since one of the research objectives of this thesis is to "create new tools to aid engineers in restoring and designing BI for coastal flood protection", NBF will be used for the remainder of this thesis but it should be noted that most existing BI are NF, not NBF.

In addition to their flood protection capabilities and increased resiliency over traditional infrastructure, NBF often have many other environmental, social, recreational, and aesthetic benefits. These are generally referred to as 'ecosystem goods and services,' and they have been discussed at length in the literature (Boyd & Banzhaf, 2007; Bridges et al., 2015; Brinson, 1993; Costanza et al., 1997; Daily, 1997; Elizabeth Murray, 2013; Fisher et al., 2009; M.E.A, 2005; Morris et al., 2018; Peter Kareiva, 2011). Ecosystem goods and services consist of any benefit an ecosystem provides that does not have a direct or tangible monetary value associated with it. Examples include habitat for wildlife, space for outdoor recreation, and pleasing aesthetics. When possible, these benefits are then assigned a monetary value in a cost-benefit analysis, so they can be more easily accounted for. However, Bridges et al. (2015) argue for a more holistic approach, where a series of established performance metrics quantify ecosystem services that are hard to quantify monetarily. In this framework, the performance metrics are evaluated alongside the cost-benefit analysis to determine the total value that a particular NBF system may provide (Bridges et al. 2015). Ecosystem goods and services may also be referred to as 'co-benefits'. This terminology can be used either to allude to the additional benefits that NBF provides over traditional infrastructure or to imply that the benefits being considered are supplementary to the primary objective of the NBF (the primary objective generally being flood risk reduction) *(*Alves et al., 2020*;* Bridges et al., 2015*;* Sutton-Grier et al., 2018*)*.

The recent adoption of NBF means its implementation faces many challenges that conventional infrastructure does not. One of the most prominent challenges is the difficulty quantifying the ecosystem goods and services NBF provides. Progress has been ongoing yet slow in this field since NBF comes in many forms, each with its own set of ecosystem goods and services. Due to these differences between varying types of NBF, uniform performance metrics cannot necessarily be applied across all forms of NBF. Instead, costs and benefits have to be quantified in unique ways for each of the ecosystem goods and services that a particular NBF provides (Bridges et al., 2015; NOAA, 2015; Sutton-Grier et al., 2018). This issue is further compounded by the general lack of research surrounding the effectiveness of NBF. While some specific combinations of NBF and ecosystem goods and services have been extensively studied, other combinations have minimal research into their efficacy or cost (Narayan et al., 2016; Oliver & Ramirez-Avila, 2019; Saleh & Weinstein, 2016; Wamsley et al., 2010). Similarly, the amount of flood protection that NBF provides varies significantly depending on the type of NBF and location and is not well studied for all forms of NBF (Narayan et al. 2016, Morris et al. 2018). Even among specific types of NBF, such as salt marshes, flood protection seems to depend on several factors that can be hard to quantify and control (Wamsley et al., 2010). Regulations in most areas are designed around conventional infrastructure, making the approval process for NBF long and arduous (Carter, 2020). However, some headway has been made with the USACE Nationwide Permit 54, allowing for the construction of living shorelines (USACE, 2017)

To address these challenges, many organizations have tried developing frameworks and best practices to help guide the design and implementation of NBF systems. This literature review has discussed or alluded to many of these frameworks (Bridges et al. 2015, NOAA 2015,

Alves 2020, Schultz et al. 2012). These frameworks quantify metrics to measure the performance of both flood risk reduction and ecosystem goods and services. However, these metrics are only helpful once an NBF has been implemented. They do not offer a way to predict the effectiveness of an NBF at reducing flooding before it has been constructed. If flood risk reduction is established as an objective, modeling is needed to predict the performance of NBF at reducing flooding at a given location.

2.3 Hydrodynamic Modeling and NBF

Two of the most advanced and widely used models in the realm of coastal flood prediction are the ADvanced CIRCulation Model (ADCIRC) and the Simulating WAves Nearshore Model (SWAN). ADCIRC is used for calculating water surface elevations and currents, while SWAN is used for computing random, coastal, wind-generated waves (Booij et al., 1996; Luettich, 2004, 1992; Westerink et al., 1994). They can be run independently or coupled (Dietrich et al., 2012; Dietrich et al., 2011). In the more than twenty years since their creation, these models have proven to be accurate, high-powered tools for predicting waves and water levels. Other similar models include Telemac and Delft3D (Galland et al., 1991; Roelvink & Van Banning, 1995; Villaret et al., 2013). Similarly, morphological models such as Xbeach have great importance and often intersect with hydrodynamic modeling (McCall et al., 2010; Roelvink et al., 2009). However, this literature review will focus on modeling techniques utilizing ADCIRC and SWAN.

2.3.1 Coastal Wetlands

While computational modeling has been used extensively to assess the characteristics of storm surge on the existing landscape, there has been much less inquiry into quantifying the

flood reduction capacity of NBF, particularly BI. One of the most studied types of NBF in terms of flood reduction is coastal wetlands.

Salt marshes are a natural barrier between populated areas and the open ocean. Questions remain about their long-term stability in the face of rising sea levels, making them a popular point of inquiry. Loder et al. (2009) examined marsh continuity, bottom friction, and marsh elevation effects on storm surge using ADCIRC. He found the level of storm surge to be inversely related to depth, bottom friction, and continuity. However, as the depth of storm surge increased, bottom friction had less of an overall effect on the surge (Loder et al., 2009). Wamsley et al. (2010) investigated the rate of storm surge attenuation that wetlands provide. Using ADCIRC, they found the level of storm surge attenuation to be highly dependent on the local landscape characteristics as well as the duration and intensity of the storm. The conclusion that salt marshes attenuate storm surge and wave action at varying rates dependent on other environmental conditions has since been expanded upon and validated (Gedan et al., 2011; Glass et al., 2018; Koch et al., 2009; Lawler et al., 2016). Similarly, other wetlands, such as mangroves, have also been found to attenuate storm surge at nonlinear rates (Zhang et al., 2012).

Others, such as Schuerch et al. (2018) have investigated how coastal wetlands are likely to change to rising sea levels. In contrast with previous studies, Schuerch et al. found that global wetland area could increase under future sea level rise scenarios if enough space was accommodated for wetland migration (Schuerch et al., 2018). Previous studies had found that coastal wetland area was likely to decrease under future sea level rise due to the inability of wetlands to accrete fast enough to keep pace with changing ocean levels (Blankespoor et al., 2014; Crosby et al., 2016).

Recently, the focus has started shifting towards the ability of constructed wetlands to reduce flooding as part of NBF systems. The Scheldt estuary, in Belgium, consists of constructed wetlands and polders used as flood storage when nearby levees overtopped. Smolders et al. (2020) found the Scheldt estuary to be able to reduce storm surge heights by up to 0.5 meters, proving the system to be effective from a flood reduction standpoint. They came to their conclusions by creating a physical scale model of the system and a digital representation of estuary in the form of a TELEMAC-3D model. They (Smolders et al., 2020)

2.3.2 Barrier Islands

Early numerical modeling studies of BI were mainly centered around their potential for flood reduction. One of the most extensive early numerical modeling studies of BI effect on depth and time of storm surge inundation was conducted by Suhayda (1997). Suhayda chose the Barataria and Terrebonne estuaries in southern Louisiana for his study area. In his study, Suhayda used the overland flooding model developed by the Federal Emergency Management Agency (FEMA) along with 7.5' and 15' resolution topographic data from USGS quad sheets and bathymetric data from the National Ocean Survey charts. The overland flooding model uses a rectangular grid for computations. Suhayda used a "fine resolution" grid with grid cells of 1,000 m^2 nearshore to get more precise water levels. Near the domain boundary, he used a grid size of 3049 m^2 to derive the forcings. He found the presence of BI slightly reduced the tidal amplitude of the back bay compared to a no BI scenario. Inversely, increasing the volume of the BI and thereby decreasing the inlet cross-sectional area slightly reduced the tidal amplitude in the back bay. However, when he looked at storm forcing, he found that the presence of BI could potentially lower surge levels in the back bay by up to 1.2-1.5 m (Suhayda, 1997).

Later, Grzegorzewski et al. (2011) conducted a similar study, investigating the effect that different BI states (natural, degraded, and restored) had on storm surge. The study area used by Grzegorzewski encompassed the Chandeleur Islands of southeastern Louisiana and Cat, Ship, and Horn Islands of Mississippi. The water levels were obtained from an ADCIRC model with a minimum grid cell resolution of 30m, and wave heights were obtained from STWAVE and SWAN with a cell resolution of 200m. Compared to the present BI scenario, restored BI could reduce significant wave heights by up to 90%, and degraded BI could increase significant wave heights by up to 495%. Similarly, they found that relative to the natural scenario, degraded BI would increase surge by 12%, and restored BI could decrease surge by 12%. The restored and degraded scenarios also affected the time of peak surge, with the restored scenario delaying the onset of peak surge by 2 hours, with the degraded scenario speeding up the onset by several hours. Other studies have concluded similar results, where BI have the potential to decrease storm surge and significant wave heights on the leeward side of the island during hurricane scenarios (Bass et al., 2018; Grzegorzewski et al., 2011; Rego & Li, 2010; Wamsley et al., 2009).

Even though BI as a means of flood reduction were the focus of early numerical modeling studies, much more work has gone into studying the morphology of BI over decadal scales. Between 2006 and 2009 Rosati et al. released a series of papers outlining a model they had developed to predict Migration, Consolidation, and Overwash (MCO) of a BI overlying poorly consolidated substrate. In these papers, they concluded that less frequent, large-scale BI restorations will reduce migration and maintain dune height better than more frequent, more minor-scale restorations (Rosati et al. 2006). They also estimated the critical cross-sectional area to reduce BI migration over a poorly consolidated substrate to be 1420 times the average surge

and wave runup combined (Rosati, 2009; Rosati et al., 2006). Other studies have agreed that when appropriately applied, beach nourishment and BI restoration can be effective in maintaining BI height and volume in the face of sea level rise (Passeri et al., 2021). Sea level rise and its effects on the morphology of BI have generally been an area of increasing interest. Using a coupled hydrodynamic and morphologic model, Passeri et al. (2018, 2020) found that Dauphin Island in Alabama had a challenging time recovering from storms under increased sea levels (Passeri et al., 2018; Passeri et al., 2020).

More recent advances have started to blur the line between hydrodynamics and morphodynamics. More evidence shows that these two fields are coupled, and each plays a significant role in storm surge characteristics. In particular, dune overtopping and overwash may account for a substantial storm surge that can impact the mainland (Cañizares & Irish, 2008; Lu et al., 2018). Additionally, sea level rise may cause landscape change that, in turn, causes changes in a region's hydrodynamic and storm surge characteristics (Bass et al., 2018; Bilskie et al., 2016).

While much is known about the storm-driven dynamics of BI, many gaps in the literature still exist surrounding BI as a means of flood protection - particularly when looking at the critical scales and configurations that achieve a significant reduction in storm surge. To this author’s knowledge, no study has attempted to create a suite of synthetic BI to test their hydrodynamic response. Instead, studies that were reviewed took existing BI and their hydrodynamic response and compared them to a theoretical scenario in which the island was either degraded or restored. Additionally, most studies reviewed on BI ability to reduce flooding took place in the Gulf of Mexico. The Gulf of Mexico is a relatively unique and complex environment. BI in other locations such as the Atlantic Coast of the United States may have different hydrodynamic and

morphologic responses than their counterparts in the gulf, even under similar storm scenarios. This makes it incredibly difficult to install new BI for flood reduction for multiple reasons. Due to the lack of worldwide data on BI hydrodynamics, it is hard to tell the effects of location on the function of BI as a form of flood reduction.

Additionally, there is no method to predict the scales and configurations at which BI become effective at providing flood reduction benefits. This may pose a significant challenge moving forward. As sea levels rise, existing BI will degrade, putting more communities at significant risk of flooding. In this reality, NBF and BI construction may become an attractive option for reducing flood risk while providing ecosystem goods and services.

CHAPTER 3 SIMULATING THE EFFECTS OF BARRIER ISLAND SCALE ON STORM SURGE ATTENUATION [1]

[1] S.D. Medlin. To be submitted to *Coastal Engineering*.

3.1 Abstract

NBF is an increasingly attractive flood reduction solution that provides additional benefits including habitat, recreation opportunities, and increased aesthetic value compared to conventional flood management infrastructure. Constructed and restored BI represent an emerging area of research within the broader field of NBF. However, information is lacking on the scales at which BI become effective for flood risk reduction. This research fills this gap by quantifying scaling relationships between BI characteristics and their flood attenuation response for a variety of synthetic storms. Data were collected from multiple sources for 16 morphological variables over more than a dozen different islands along both the Gulf and Atlantic coasts of the United States and compiled into a single database. This database was used to generate idealized models of coastal landscapes containing BI. These idealized landscapes were combined with synthetic storm surge forcings as inputs to the ADvanced CIRCulation model (ADCIRC). In a series of experiments, BI dune height and length, inlet cross sectional area, and distance from the BI to mainland were all individually adjusted to determine their effects on storm surge inundation. BI reduce maximum water elevations by up to 60%. These results will help encourage maintenance and creation of BI as flood protection infrastructure.

3.2 Introduction

Coastal communities along the Gulf and Atlantic Coasts of the United States are subject to storm surges from strong wind conditions (McCabe et al., 2001). Tropical cyclones and their associated surges are among the most severe natural disasters regarding monetary cost and loss of life (Smith et al., 2021). As the climate continues to change, tropical cyclones may increase in intensity due to increased temperature and moisture in the atmosphere (Arias et al., 2021). Additionally, the effects of tropical cyclones will be felt more acutely as sea levels rise and affect

larger populations and more property. Traditionally, coastal flooding has been mitigated with conventional (grey) flood infrastructure such as levees, seawalls, and breakwaters. However, it has become increasingly necessary to design infrastructure that works alongside nature to increase habitat, resilience, recreational opportunities, and other co-benefits while also providing flood protective benefits. This necessity culminated in the creation of the Network for Engineering with Nature® program (N-EWN) (*Network for engineering with nature*, 2022). N-EWN aims to increase the use of natural infrastructure through research, education, and outreach. As part of this initiative, emphasis has been placed on determining the spatial scales necessary for natural infrastructure to be effective for flood attenuation in coastal and riverine areas.

While BI are common worldwide, research into their flood attenuation abilities is limited. One of the first studies that quantified the effect of BI on water surface elevation found restored islands with higher dunes and smaller cross-sectional inlet areas provide the Terrebonne and Barataria estuaries with the highest degree of storm surge protection (Suhayda, 1997). Recent studies compared the existing BI conditions to potential degraded conditions in Louisiana (Wamsley et al., 2009), Mississippi (Grzegorzewski et al., 2009), and Texas (Bass et al., 2018) and found a 5 to 15% reduction in maximum water elevations. These studies face the same limitations of focusing on "real-world" BI examples in the Gulf of Mexico. Thus, the applicability of their findings is restricted to similar topographic/bathymetric conditions.

The research presented in this paper develops scaling relationships between BI morphological characteristics and resulting flood responses using a hydrodynamic model for various synthetic storm surge events. To the author's knowledge, this is the first idealized study of how the spatial scales of BI affect their ability to attenuate storm surge induced flooding. The broad nature of this study allows the scaling relationships outlined in this work to be applied in

more regions than results in previous studies. These relationships will give engineers and practitioners confidence in designing and recommending constructed or restored BI as an effective form of flood mitigation infrastructure.

3.3 Methods

3.3.1 Data

Spatial characteristics of BI was collected for 16 morphological parameters over 23 islands along the Gulf of Mexico (GOM) and Atlantic coasts of the United States. These data were obtained from multiple sources, including United States Geological Survey (USGS) 3D Elevation Program (3DEP) digital elevation models (DEM), and existing databases (Doran, 2017; Mulhern et al., 2017; Murshid & Mariotti, 2021). All variables and data sources are summarized in Table 1.

These variables were identified based on their ability to describe the position and sizing of BI systems at the landscape scale. Individual BI were selected based on data availability and the level of anthropogenic influence on the island's landscape. Anthropogenic factors can have an outsized impact on BI topography and morphology, which is outside the scope of this study (Kratzmann & Hapke, 2010). Additionally, this study aims to model natural island scenarios, rather than the entire range of technically feasible scenarios, to lay the groundwork for future engineering guidance on this subject. For these reasons, every island must have at least 30% of its length uninhabited or otherwise protected (e.g., state park, national seashore, national monument, wildlife refuge, or private nature reserve). All Louisiana BI were excluded from consideration due to the unique geomorphology of the Mississippi River delta. 23 BI across five states were included in the database (Table 3.2). The selected islands represent a broad range of island conditions along the Gulf of Mexico and Atlantic coastlines. The median of each BI

variable determined a baseline (or ideal) BI. Multiple BI configurations were created starting from the baseline condition to cover a broad range of potential BI scenarios.

Table 3.1: Morphological variables collected and their sources

Parameter	Median	Data Source	Reference
Dune Crest Height	3.18 m	Variables pulled from an existing web database. Authors of the database source data from various Lidar surveys	(Doran, 2017)
Dune Toe Height	2.04 m		
Beach Width	46.42 m		
Slope	.0243		
Distance to Vegetation	63.96 m		
Estimated Length	14.64 km	Sourced from existing database. Database authors sourced their data from aerial imagery.	(Mulhern et al., 2017)
Estimated Width	1.08 km		
Island Area	16.0 km^2		
Island Perimeter	40.62 km		
Width of Continental Shelf	139.95 km		
Depth of Closure	3.62 m		
Minimum Inlet Width	2.40 km	Variables pulled from existing database. Database authors sourced their data from NOAA navigational charts.	(Murshid & Mariotti, 2021)
Maximum Inlet Depth	13.29 m		
Mean Inlet Depth	5.35 m		
Distance from Island to Mainland (range)	2.90 km	Calculated from USGS 3DEP DEM's	Collected as part of this thesis

Table 3.2: Islands Represented in the Database

Island Name	State	Coastline
Cat Island	Mississippi	Gulf Coast
East Ship Island[1]		
West Ship Island[1]		
Horn Island		
Petit Bois Island		
Dauphin Island	Alabama	
Perdido Key	Florida	
Santa Rosa Island		
St. Vincent Island		
Little St. George Island[2]		
St. George Island[2]		
Dog Island		
Cumberland Island	Georgia	Atlantic Coast
Little St. Simon's Island		
Sapelo Island[3]		
Blackbeard Island[3]		
St. Catherine's Island		
Ossabaw Island		
Wassaw Island		
Shackleford Banks	North Carolina	
South Core Banks[1]		
North Core Banks[1]		
Portsmouth Island		

[1] Data from East/West Ship island and North/South Core Banks were combined in the database as they have been reconnected

[2] Little St. George and St. George Island were combined as they naturally existed as a single island, but were separated by a small, manmade channel.

[3] Blackbeard Island and Sapelo Island were combined in the dataset as not all data sources considered them separate islands.

3.3.2 Coastal Landscape Generator

A MATLAB script was developed to automate the creation of idealized coastal landscapes (Medlin, Hewageegana, et al., 2022). The script collects user input on the size, shape, location, and number of BI. It generates a matrix of georeferenced elevation points that describe the topography and bathymetry of the BI and surrounding region. The program can produce a single or several landscapes given the input parameter space.

To generate the idealize BI landscapes, the program first creates a baseline cross-shore transect from the user-supplied information. Next, an existing BI transect is imported. The landscape is scaled according to user-specified dune height and island width, and is superimposed to the baseline profile. The resulting cross shore transect is then used for the width of the domain to create a uniform landscape in the longshore direction. Finally, inlets are inserted into the profile at user-specified widths, depths, and intervals.

3.3.3 Hydrodynamic Model

All numerical simulations were conducted using the ADvanced CIRCulation (ADCIRC) model (Luettich, 2004, 1992). ADCIRC is a large-scale, finite element, hydrodynamic modeling framework. It utilizes the depth-averaged shallow water equations to solve for water levels and depth-averaged velocities. ADCIRC has been widely used to simulate tides and storm surges (Bilskie et al., 2016; Dietrich et al., 2012; Dietrich et al., 2011; Westerink et al., 2008).
An unstructured mesh with a semi-circular ocean boundary extent was used in all ADCIRC simulations (Figure 3.1). The mesh has a radius of approximately 80 km and contains 196,968 nodes and 391,692 elements. The minimum element size is 100 m at the mainland boundary and increases linearly to 1 km as it moves further offshore. The mesh ranges between approximately 150 m and 200 m in resolution at the location of the BI. To accommodate different BI

landscapes, elevations from the landscape matrices, generated by the Landscape Generator MATLAB script (Section 3.3.2), were interpolated to the mesh nodes. A different landscape matrix was used whenever new topobathy was required. Interpolating different landscape matrices onto the same mesh allowed the positioning of mesh nodes and element connectivity to remain static between all simulations. Keeping mesh node positioning and element connectivity static eliminated the risk of biasing the results due to differences in the underlying mesh.

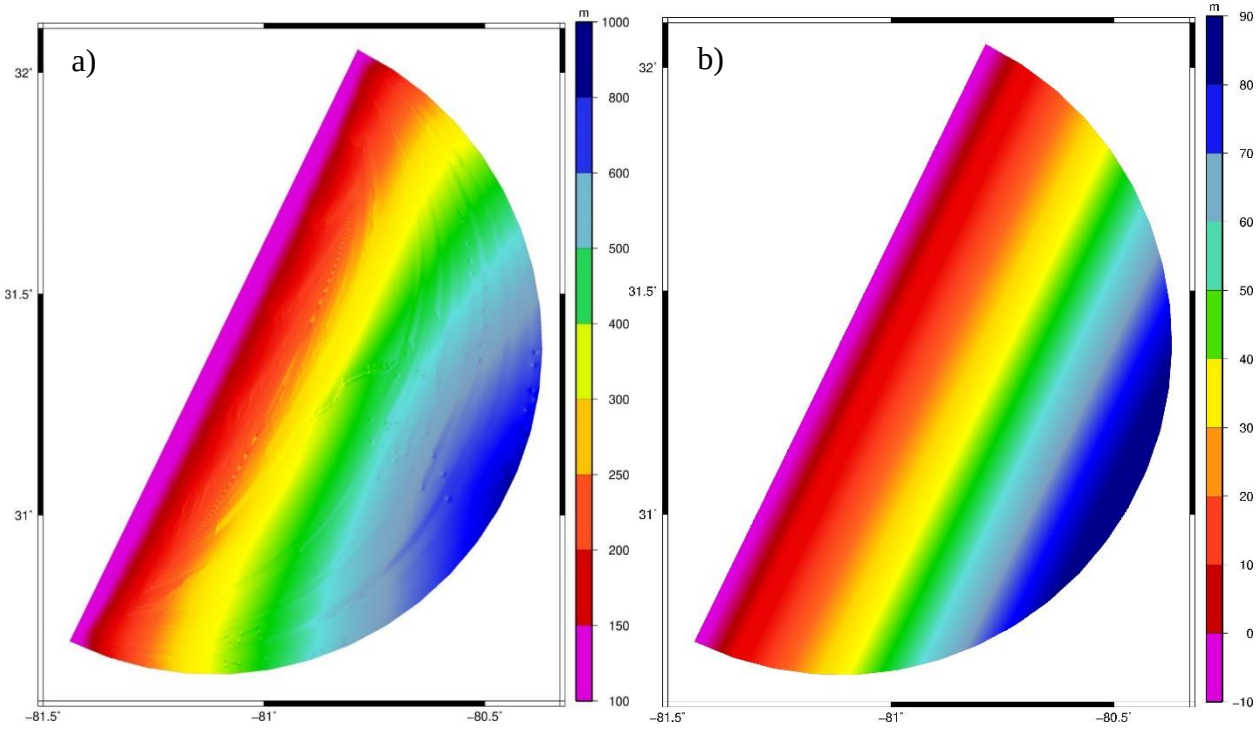

Figure 3.1: a) Grid Size and b) Bathymetry (depth is positive) of the control mesh used in simulation experiments.

3.3.4 Forcing

A large-scale North Atlantic tidal simulation was run in ADCIRC over an arbitrary 10-day period to find relevant tidal information. The domain for this simulation included the entirety of the North Atlantic Ocean, Caribbean Sea, and the Gulf of Mexico, westward of the 60th Meridian West. The previously developed 53K mesh was used in this simulation. This mesh had 52,774 nodes and 98,365 elements ranging from approximately 1.7 km to 120 km in size (Hagen

et al., 2006). The position of the ocean boundary nodes from the detailed mesh described in Section 3.4 were used as recording stations in this tidal simulation. Amplitude and phase information for all harmonic tidal constituents were found at each boundary node recording station. This information is time invariant, so the length of the simulation had no bearing on the results. From these results, a constant-amplitude, semidiurnal, sinusoidal, M2 tidal signal was reconstructed for each node along the ocean boundary in the detailed mesh. This method allowed the authors to pick a tidal amplitude for analysis (in this case 1 m) and scale that amplitude to each node along the mesh boundary, keeping the relative difference in amplitude along the boundary the same as what would be found if the mesh were physically located offshore. For this analysis, the mesh was placed offshore of coastal Georgia. A 1 m tidal signal was chosen as it is a realistic tidal amplitude for coastal Georgia, and it eases visualization of depth of inundation above Mean High Water.

Storm surge hydrographs were then superimposed onto the idealized M2 tidal signal. Six different storm surge hydrographs were developed. These hydrographs represented either a "fast" or "slow" moving storm and had amplitudes of 1 m, 2 m, and 4 m. These values were chosen based on an analysis of SURGEDAT data (Needham & Keim, 2012).

Every SURGEDAT entry had an assigned confidence level from one to five. In this analysis, confidence levels of two or greater were used. This confidence level corresponded to at least one anecdotal source from the area of peak surge or one scientific source that conflicted with credible anecdotal accounts or other scientific sources. Greater confidence levels corresponded to one or more credible scientific sources with no contradictions.

Surge events in the Gulf of Mexico or Atlantic Coasts of the United States with a confidence level of two or greater had a median surge of 1.5 m with a standard deviation of 1.2

m. The surge events were skewed to the right (surge events of greater magnitude). 83.17% of all surge events fell between 1 and 4 meters in amplitude with 10.89% of surge events below 1 m, 5.94% of surge events greater than 4 m, and 0.73% of events greater than 6 m in amplitude. As this study was primarily concerned with flooding impacts, surges of amplitudes smaller than 1 m were not of importance in this analysis. Based on this data, four surge amplitudes were chosen for inclusion in the simulated hydrographs; 1 m, 2 m, 4 m, and 6 m. The fast hydrographs had a peak surge duration of approximately 8 hours while the slow hydrographs had a peak surge duration of approximately 24 hours. The shape of the hydrographs was determined by modifying the equation found in Xu et al. (2010).

$$H_t(t) = \begin{cases} H_t(t) = H_P\left(1 - a \times e^{-\left|b/(t-t_0)\right|}\right) for\ rising\ limb \\ H_t(t) = H_P\left(1 - c \times e^{-\left|d/(t-t_0)\right|}\right) for\ falling\ limb \end{cases} \quad (3.1)$$

Where $H_t(t)$ was the surge, in meters, at a given time, t (hours). H_P was the peak surge in meters. t_0 was the time of landfall, in hours from the start of the simulation, and a, b, c, and d were constants. For this analysis, the constants a, b, c, and d were set such that the rising limb and falling limb were the same shape, creating a symmetrical storm. a and c were set to 0.9 and b and d varied based on the hydrograph shape. The 8, 12, and 24-hour peak hydrographs had both b and d set to 1.5, 3, and 6, respectively. These hydrographs were then superimposed onto the tidal forcing to get the entire tide and storm surge signal. The peak storm surge was timed to coincide with high tide to represent a worst-case scenario.

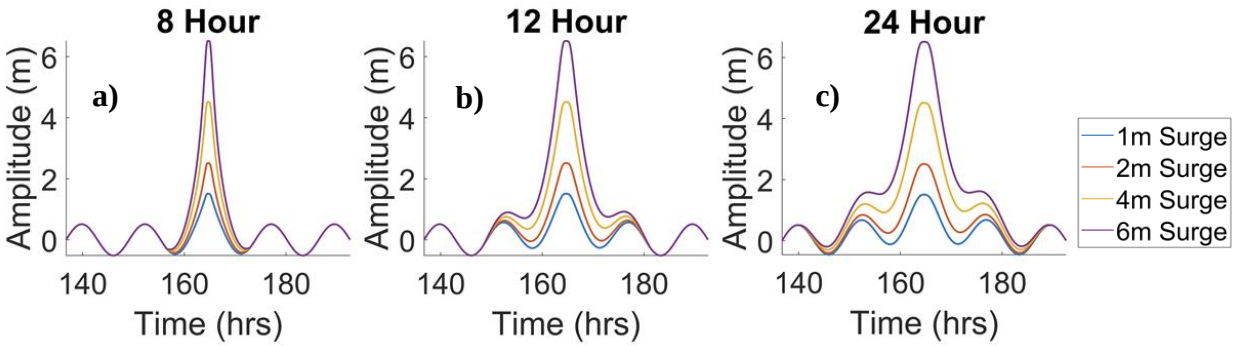

Figure 3.2: a) forcing for 8-hour duration storm, b) 12-hour duration storm, and c) 24-hour duration storm.

3.3.5 Experiments

Using the above boundary forcings and landscape generation script, two experiments were conducted. The first experiment varied the number of tidal inlets and the foredune height in a 128 km long section of BI. The inlets were 5.35 m deep and 2.4 km in width, which were the median values found in the data. The number of inlets varied from 0-6. The heights of the foredune were 2.07 m, 3.29 m, and 4.51 m which represent the mean of the data and the mean +/- one standard deviation. All 12 of the boundary forcings were used. Additionally, a control scenario was run with all 12 boundary forcings and the same bathymetry as the other simulations but without any islands present. A total of 252 simulations were ran for this experiment in addition to the 12 control simulations.

The 2nd experiment kept the number of tidal inlets constant while varying their width. Inlet widths were set to 300 m, 500 m, 700 m, 900 m, 1900 m, 2900 m, 4900 m, and 6900 m. All other variables were set to the same values as the first experiment. The same control scenarios were used for comparison. A total of 288 simulations were performed for this experiment.

Both experiments simulated one day of model spin up followed by 9 days of tidal and storm surge forcing. Peak surge was timed to occur at high tide approximately 165 hours into the simulation. Peak surge duration was determined by the forcings shown in Figure 3.2. A one

second timestep was used in all simulations. Bottom friction was set to a constant Manning's *n* value of 0.025. No morphodynamic changes were simulated.

3.4 Results

3.4.1 Explanation of Results

In both experiments, water levels were recorded every 15 minutes at each node in the model domain. The peak water level along the mainland 1 m contour was then extracted for all simulations. This water level was used to make maximum water level comparisons between simulations. The 1 m contour was used to represent the lowest likely elevation that major infrastructure and housing investments would be made. Comparisons of water levels at exact locations between simulations were not made as peak water levels shifted with the locations of inlets.

To compare results from the first and second experiments, data were parameterized by the ratio of total linear inlet width to island length as:

$$Ir = \frac{\sum_{i=1}^{n} w_i}{\sum_{i=1}^{n} l_i} \qquad (3.2)$$

Where *Ir* is the Inlet Ratio, w_i is the width of inlet *i*, and l_i is the length of island *i*. *Ir* accounts for both the width of each inlet and the overall quantity of inlets in the domain.

The amount of attenuation seen varied drastically depending on the specific island configuration tested. Only 58.1% of scenarios saw a decrease in peak water levels. The remaining simulations, 41.9%, saw a slight increase in peak water levels. This increase was observed to be up to 12.1% above the maximum water surface elevation observed in the control scenario. Maximum modeled attenuation was 61.2%. A histogram of observed attenuations can be seen in Figure 3.3.

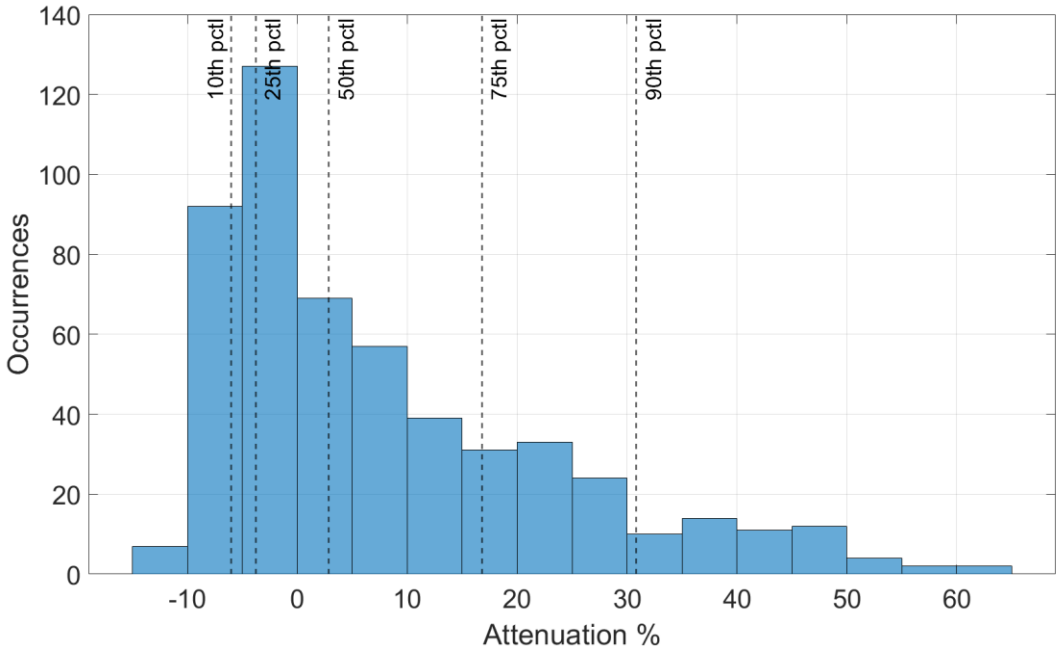

Figure 3.3: Histogram of modeled reductions in peak water surface elevation (%) along the 1 m contour. 10^{th}, 25^{th}, 50^{th}, 75^{th}, and 90^{th} percentiles are called out as dashed vertical lines.

3.4.2 Effect of Inlet Ratio and Dune Height

Figure 3.4 shows the percent reduction in maximum water levels along the mainland 1 m contour for various inlet ratios, dune heights, and surge signals. Similar plots for all 12 storm surge forcings can be found in Appendix B. Generally, smaller inlet ratios lead to larger reductions in peak water levels. In the best-case scenario, an inlet ratio of 0.0 (A single island with no inlets), a dune height of 4.51 m, a surge amplitude of 2 m, and a duration of 8 hours, the BIs were able to reduce peak water levels by 58.1% or about 1.16 m. Similarly, peak water level reductions of 35.1% or 1.40 m were observed with an inlet ratio of 0.0 (A single island with no inlets), dune height of 4.51 m, and a surge signal with an amplitude of 4 m and duration of 12 hours. However, surge attenuation did not scale linearly with inlet ratio and was dependent on other factors such as dune height and surge duration.

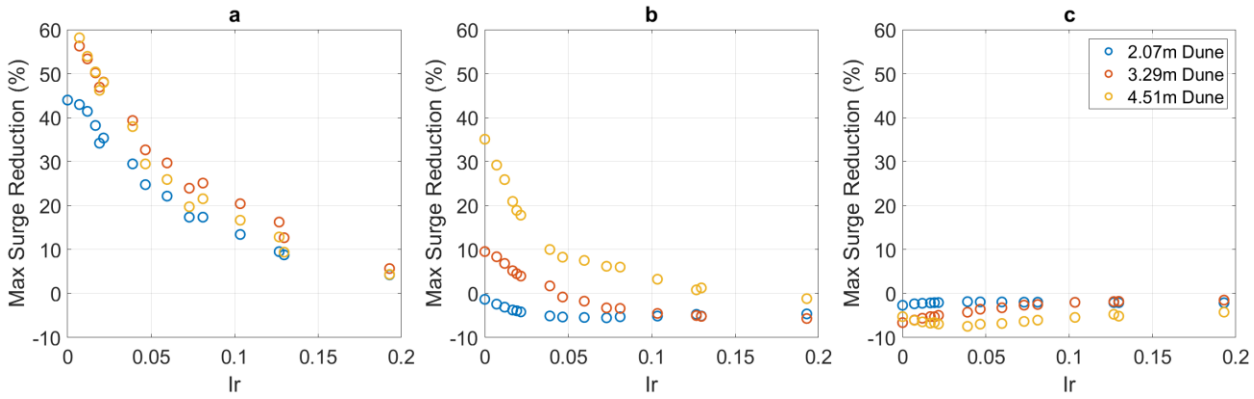

Figure 3.4: Effect of Inlet Ratio on maximum water levels for various peak dune heights and storm surge with a) 2 m amplitude and 8-hour duration, b) 4 m amplitude and 12-hour duration, c) 6 m amplitude and 24-hour duration.

Dune height played a key role in determining the surge attenuation a given BI configuration would provide. In particular, a dune needed to be at least as tall as the storm surge to provide maximum flood protection benefits. Simulations in which storm surge overtopped the dune generally saw significantly less storm surge attenuation (-0.47 m – 1.34 m of attenuation) than simulations where the dune height was greater than the peak surge height (-0.12 m – 1.92 m of attenuation). Once the dune reached a sufficient height to prevent overtopping, further increases to dune height appeared to provide little to no additional flood attenuation benefits.

3.4.3 Effect of Surge Duration

Storm duration had a significant effect on how well BI were able to attenuate surge. As seen in Figure 3.5, the ability of a particular BI system to defend against an incoming surge depended largely on the duration of the surge event as well as the inlet ratio of the BI system. Systems with smaller inlet ratios (< 0.1) tended to be better at attenuating short duration storms. While systems with larger inlet ratios (>0.1) tended to be better at attenuating longer duration storms. However, this was not always true. In Figure B.5, all BI systems with a 3.29 m dune

height were able to attenuate a short (8-hour) duration surge event most effectively, with smaller inlet ratios providing the most protection.

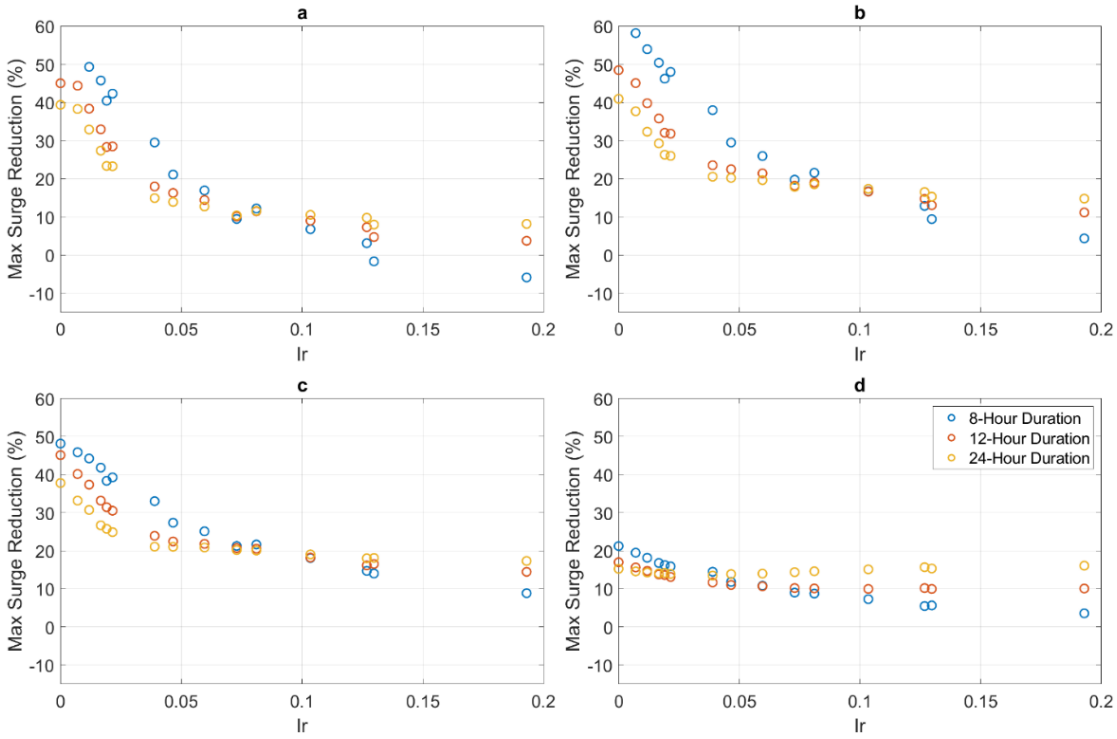

Figure 3.5: Inlet Ratio vs maximum water levels for a 4.51 m dune over various storm surge durations and surges with a) 1 m amplitude, b) 2 m amplitude, c) 4 m amplitude, and d) 6 m amplitude.

3.5 Discussion

3.5.1 Scale Consolidation/Power Functions

In Sections 3.4.2 and 3.4.3, the effects of inlet ratio, dune height, surge amplitude, and surge duration were all discussed in terms of how each parameter independently affected BI flood attenuation capabilities. These parameters were consolidated into a single prediction feature to create a more holistic understanding of how BI systems can reduce storm surge-induced flooding and to provide a practical tool for engineering practitioners and stakeholders.

$$pred = \frac{(h_d/a_s)^{exp1}}{Ir^{exp2} * T_s^{exp3}} \quad (3.2)$$

Where 'pred' is the predictor feature, h_d is the dune height in meters, a_s is the surge amplitude in meters, T_s is the surge duration in hours, and exp1, exp2, and exp3 are the three exponents outlined in Table 3.3. The values of each exponent were optimized through the Nedler-Mead simplex algorithm (Lagarias et al., 1998). The curves fitted to the data were a two-term exponential function for 1 m and 2 m surge response, and a three-term polynomial function for the 4 m and 6 m surge response. These equations had r^2 values of 0.925, 0.918, and 0.903, respectively. Equations for each of the fits can be found on Figure 3.6-3.7.

Table 3.3: Exponents for the predictor function given different surge amplitudes

	Exponent 1	**Exponent 2**	**Exponent 3**
1 m Surge	-0230.	0.815	1.270
2 m Surge	0.352	0.518	1.280
4 m and 6 m Surge	0.247	0.056	0.278

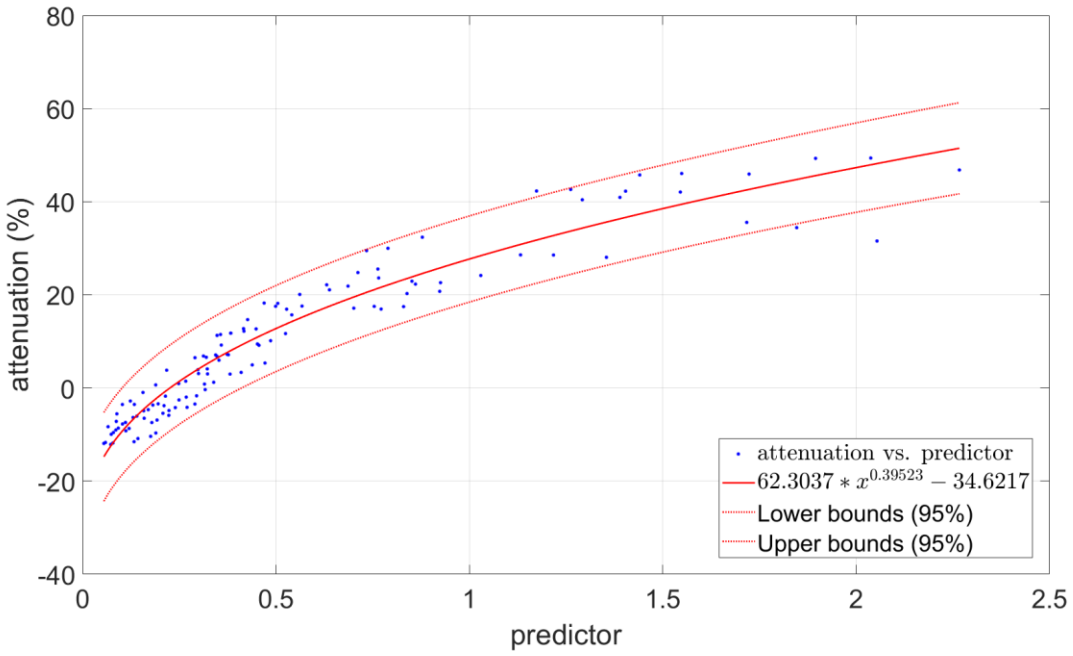

Figure 3.6: Plot of the prediction feature vs. % attenuation for 1 m surge.

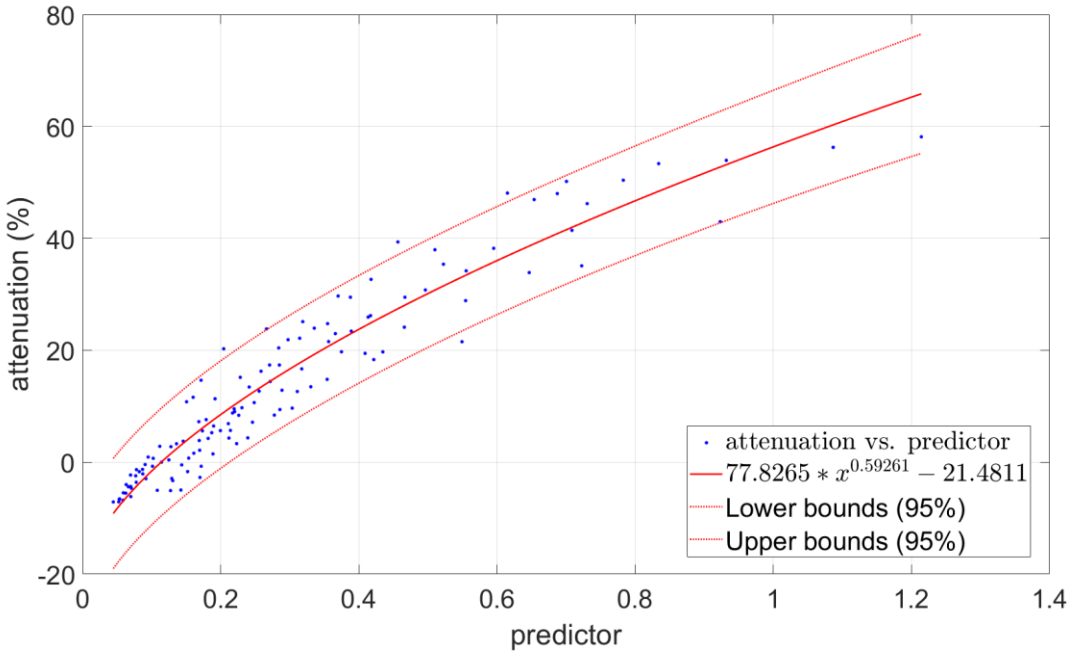

Figure 3.7: Plot of the prediction feature vs. % attenuation for 2 m surge

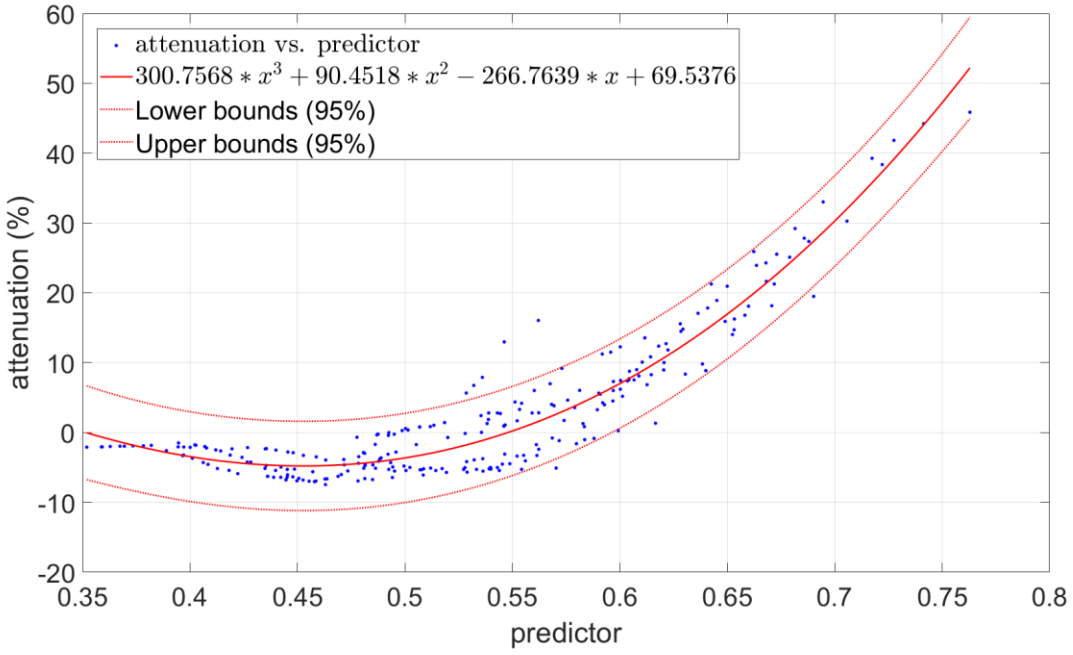

Figure 3.8: Plot of the prediction feature vs. % attenuation for 4 m and 6 m surges.

3.5.2 Comparison of Idealized vs. Actual BIs

This study did not model any real-world BI systems, so it is important to ensure the idealized systems modeled represent actual conditions found in nature. This was partly addressed through the compilation of the BI parameter database. However, since the median of each parameter in the database was used to form the landscapes, it is possible that the generated landscapes are merely a theoretical "median" island with no natural equivalent. This section attempts to address this question with three example BI systems.

Padre Island, along the southern Texas coast, is representative of the largest BI modeled in this study. Padre Island is approximately 120 km long and ranges in width from ~1.8 km - 3.5 km, with an average width of 2.3 km (Mulhern et al., 2017) and a distance from the mainland of ~2.5 km - 6 km. This is similar to the longest idealized island simulated in this study at 128 km. All the study's islands were placed 5.5 km from the mainland, within the range that Padre island sits. Additionally, the width of all simulated islands was 2.4 km, within 5% of the average width of Padre Island. Dune heights on Padre island vary greatly (2 m-16 m) but average ~3-5 m in height. Padre island differs from the simulations presented in this study in terms of the width of its inlets. On the island's north side, Packery channel is 80 m in width, and the pass on the island's south side is approximately 180 m in width. Both channels are smaller in width than those tested in this study. However, both of these channels are engineered channels. The data used in this study was not meant to be representative of them, as the data collected was from natural single-threaded inlets as defined in Murshid et al. (2021). The nearest naturally occurring channel is Aransas pass. This channel has been stabilized by dredging, but was formed by natural processes. It is approximately 380 m in width, within the range of channels incorporated in the idealized landscapes. A comparison between Padre Island and the largest simulated island can be seen in Figure 3.9.

Portsmouth island in the North Carolina Outer Banks is representative of the medium-sized idealized islands modeled in this study. Portsmouth Island has an approximate length of 29.4 km and a width ranging from 0.4 m – 3.3 km. The median dune crest is 3.39 m in height, only 10 cm greater than the middle (3.29 m) dune crest option modeled. The distance to the mainland gradually gets further from south to north until the mainland gives way to the Pamlico Sound at the island's northern half. At the southern end, the mainland is 2.9 km from the back side of the island. Just before the mainland gives way to the Pamlico sound, the island is 6 km from the mainland. At the northernmost end, after the Pamlico sound opens up, Portsmouth Island is 29.7 km from the mainland.

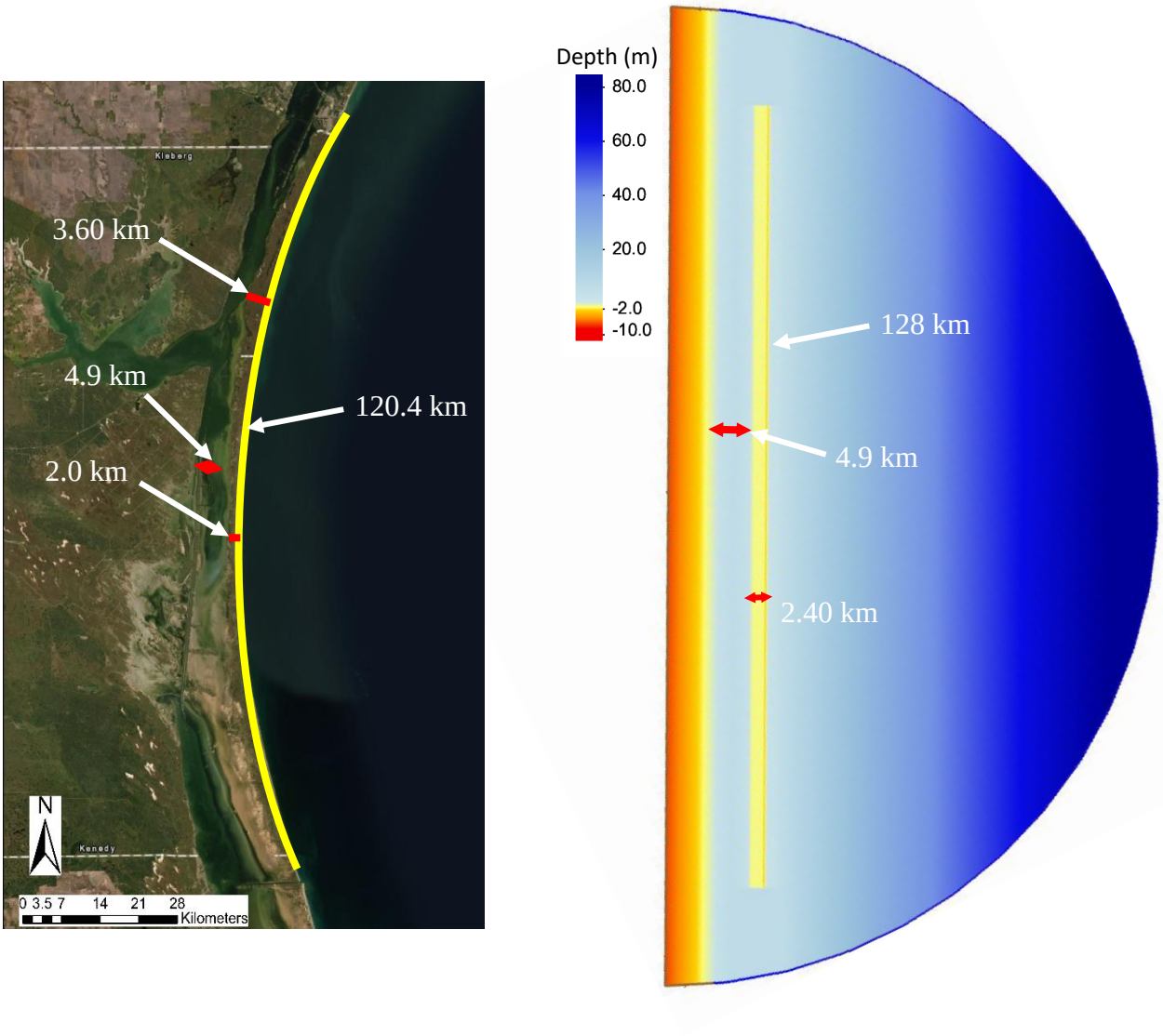

Figure 3.9: Length and width of Padre Island, Texas (left) compared with largest simulated idealized island (right)

St. Catherine's Island is representative of the smaller islands modeled in this study. St Catherine's Island is approximately 16 km in length, the same as the smallest idealized islands modeled in this study, and between 2 km - 5.3 km in width. The median dune height of St. Catherine's Island is 2.19 m, 12 cm taller than the shortest dune option modeled (2.07 m). The largest difference between St. Catherine's Island and the hypothetical islands modeled in this

study is St. Catherine's Island only sits between 0.2 km - 1.9 km from the mainland. This is a significantly shorter distance than the 5.5 km modeled for all islands in this study.

The comparisons presented in this section indicate the idealized BI geometries modeled in the previous hydrodynamic simulations are a reasonable approximation of the range of variability present in natural BI along the Gulf and Atlantic coasts of the U.S. This is important as BI whose form mimics that found in nature may exhibit greater long-term morphodynamic stability than islands with a form driven by anthropogenic impacts (Magliocca et al., 2011; Miselis & Lorenzo-Trueba, 2017; Rogers et al., 2015).

3.5.3 Limitations and Future Work

There are several areas where the accuracy and validity of this work can be improved. Several groups collected the data in the BI database at different points of time and at different spatial resolutions and accuracy. It is possible that the entire range of BI possibilities was not captured in the data used to inform the modeling efforts.

The authors did not have the time or resources to model every possible BI configuration. In particular, future simulations which vary the distance between the BI and the mainland are needed to gather a complete picture of how BI systems attenuate floods. Similarly, a constant Manning's *n* value was used to simulate a sandy, uninhabited, unvegetated BI. In reality, BI are often vegetated or inhabited, so more experiments adjusting friction factors are needed.

Finally, morphology changes over the surge event were not considered. It has been shown that BI morphology can change dramatically over the course of the storm, particularly in the case of overwashing (Houser et al., 2008; Masselink & van Heteren, 2014). As the dune gets overwashed, its elevation decreases, thereby increasing the depth of inundation over the BI, allowing more water to escape after the storm event than a similarly sized static floodwall. Since

this study did not model this morphological change, some simulations where the dune was overwashed may show less attenuation than in the real world, as the onshore pressure gradient may be pumping water into the back bay. However, once the pressure gradient subsides, the dune is still in place, and all water must drain through the inlets. This may be the cause of increased water levels seen over long-duration surge events paired with tall dune heights. Similar dynamics have been studied in closed and fringing reef systems (Lowe et al., 2009; Lowe et al., 2010)

3.6 Conclusion

BI have received increasing interest as an alternative to traditional (gray) flood mitigation infrastructure in coastal areas. However, few studies have attempted quantified BI flood attenuation abilities, and no previous studies have systematically examined a wide range of conditions using an idealized modeling framework. This work fills that research gap by compiling a BI morphological features database and using it to inform a suite of hydrodynamic storm surge simulations on idealized coastal and BI landscapes.

BI generally attenuate the most flooding with a low inlet width to island length ratio, a dune height tall enough to prevent overtopping, and during short duration surge events. In these circumstances, BI can reduce peak water levels by up to 58% compared to a baseline scenario with no BI; however, this attenuation level is rare as the attenuation provided by a BI system drops off rapidly as the inlet ratio increases. Additionally, if the dune crest is not tall enough to prevent overtopping, attenuation drops off significantly based on the depth of inundation above the dune crest. Once the dune is sufficiently tall to prevent overtopping, little to no additional flood reduction benefits are gained from making it taller.

In addition to the BI itself, the duration of the surge event plays a large role in surge reduction. Islands with smaller inlet ratios are generally more effective at attenuating short

duration surge events, while inlets with larger inlet ratios are generally more effective at attenuating long-duration surge events.

This study also created a prediction feature to consolidate surge Inlet Ratio, surge duration, and dune height, and surge magnitude into a single factor to predict the overall effectiveness of a BI system at attenuating floods. The equation for the prediction feature can be found in equation 3.2. The overall structure of the prediction feature equation was constructed based on observed attenuation patterns among different BI landscapes. For example, Inlet Ratio was observed to be inversely correlated to the flood attenuation provided by the BI so it was placed in the denominator of the equation. The exponents of the prediction feature equation were found using the Nedler-Mead Simplex algorithm. Three curves were then fit the prediction feature vs. % of flood attenuated based on surge magnitude. The prediction feature and associated curves can be used to predict the level of flood attenuation that different BI configurations can provide.

While more work is needed to develop a truly holistic understanding of how different BI systems can mitigate flooding from surge events, this research lays the groundwork for future inquiry into this subject and has provided a useful flood prediction tool for basic BI landscapes. This work has also created an open database and scripting tools available to the general public via GitHub.

CHAPTER 4 CONCLUSIONS

4.1 Significance

This work is the first of its kind in that no other study has attempted to use a wholly idealized hydrodynamic model to describe BI abilities to attenuate flooding. All other numerical modeling studies compared theoretical (degraded/restored) scenarios to existing BI conditions in select locations in the Gulf of Mexico and New York. The prediction feature described in Section 3.5.1 is the first known tool to predict BI flood attenuation performance based on a BI's scale and incoming surge characteristics. With an accuracy of +/-8% this tool will be valuable in preliminary design decisions. Additionally, while more work needs to be completed to truly understand how BI can be used for flood attenuation, all the tools, scripts, and data used in this study are freely available to the public. This will allow accelerated research on this topic in the future.

4.2 Future Work

There are several areas where this research can be improved upon in the future. These improvements fall into three general categories.

1. More simulation complexity
2. Increased data and parameters in morphology database
3. Further analysis of existing results

There are several parameters in which data were assembled but did not get modeled due to time or computational limitations. The most promising next steps in model complexity are varying the distance between the island and the mainland, accounting for friction coefficients

between vegetated/un-vegetated and inhabited/uninhabited, and modeling changes in dune morphology over the course of a storm event. Accounting for these factors may increase the precision of the prediction factor, moving closer to a holistic understanding of BI flood attenuation performance. In particular, modeling dune evolution over the course of a storm event seems promising.

While data were collected on 23 BIs and 15 parameters for this research, there are hundreds of BI in the U.S. and thousands around the world. Adding more data to the BI morphology database may provide insight into different modes of BI morphology. Specifically, there is a need to add beach characteristics (Dune Crest Height, Dune Toe Height, Beach Width, Beach Slope, and Distance to Vegetation) for more islands. Adding new parameters to the database may prove equally as valuable.

While this thesis analyzed relative attenuation between simulations and their controls, more analysis can be done with existing simulations and their data. Measuring volumes of water flowing through inlets vs over overwashed BI may provide valuable insights into where water is entering the back-bay system. Similarly, studying depth of inundation may prove valuable for engineers trying to optimize for minimal inundation time, rather than minimum depth of inundation. More broadly, analyzing average attenuation in a back-bay system and comparing it to the maximum attenuation may show how sensitive attenuation is to the location of the BI.

4.3 Conclusions

It was found that BI are capable of reducing the maximum depth of surge inundation by up to 58%. The amount of attenuation seen depended on all three factors set out in Research Question 2: BI scale, BI configuration, and storm characteristics. For this reason, we were unable to find a singular island combination that provided maximum flood reduction in all scenarios.

In conducting this research, we were able to develop a suite of MATLAB scripts that are available to the public via GitHub. These scripts streamline the process of pre and post processing simulations of BI within ADCIRC (Medlin, Santiago-Collazo, et al., 2022). Additionally, we compiled a database of BI morphological parameters that is freely available to the public (Medlin & Bilskie, 2022).

WORKS CITED

Alves, A., Vojinovic, Z., Kapelan, Z., Sanchez, A., & Gersonius, B. (2020). Exploring trade-offs among the multiple benefits of green-blue-grey infrastructure for urban flood mitigation. *Science of The Total Environment, 703*, 134980. https://doi.org/10.1016/j.scitotenv.2019.134980

Arias, P. A., Bellouin, N., Coppola, E., Jones, R. G., Krinner, G., Marotzke, J., Naik, V., Palmer, M. D., Plattner, G. K., Rogelj, J., Rojas, M., Sillmann, J., Storelvmo, T., Thorne, P. W., Trewin, B., Achuta Rao, K., Adhikary, B., Allan, R. P., Armour, K., . . . Zickfeld, K. (2021). Technical summary. In V. Masson-Delmotte, P. Zhai, A. Pirani, S. L. Connors, C. Péan, S. Berger, N. Caud, Y. Chen, L. Goldfarb, M. I. Gomis, M. Huang, K. Leitzell, E. Lonnoy, J. B. R. Matthews, T. K. Maycock, T. Waterfield, O. Yelekçi, R. Yu, & B. Zhou (Eds.), *Climate change 2021: The physical science basis. Contribution of working group i to the sixth assessment report of the intergovernmental panel on climate change* (pp. 33−144). Cambridge University Press. https://doi.org/10.1017/9781009157896.002

Arnell, N. W. (1984). Flood hazard management in the united states and the national flood insurance program. *Geoforum, 15*(4), 525-542. https://doi.org/10.1016/0016-7185(84)90023-x

Arnold, J. L. (1988). *The evolution of the 1936 flood control act*. (EP 870-1-29). Fort Belvoir, Virginia

ASCE. (2016). *Failure to act*. https://dx.doi.org/10.1061/9780784481387

Bass, B., Torres, J. M., Irza, J. N., Proft, J., Sebastian, A., Dawson, C., & Bedient, P. (2018). Surge dynamics across a complex bay coastline, galveston bay, tx. *Coastal Engineering, 138*, 165-183. https://doi.org/https://doi.org/10.1016/j.coastaleng.2018.04.019

Bergsma, E. (2018). Expert-influence in adapting flood governance: An institutional analysis of the spatial turns in the united states and the netherlands. *Journal of Institutional Economics, 14*(3), 449-471. https://doi.org/10.1017/s1744137416000552

Bilskie, M. V., Hagen, S. C., Medeiros, S. C., Cox, A. T., Salisbury, M., & Coggin, D. (2016). Data and numerical analysis of astronomic tides, wind-waves, and hurricane storm surge along the northern gulf of mexico. *Journal of Geophysical Research: Oceans, 121*(5), 3625-3658. https://doi.org/10.1002/2015jc011400

Blankespoor, B., Dasgupta, S., & Laplante, B. (2014). Sea-level rise and coastal wetlands. *AMBIO, 43*(8), 996-1005. https://doi.org/10.1007/s13280-014-0500-4

Booij, N., Holthuijsen, L. H., & Ris, R. C. (1996). The "swan" wave model for shallow water. *Coastal Engineering Proceedings*, *1*(25). https://doi.org/10.9753/icce.v25.%p

Boyd, J., & Banzhaf, S. (2007). What are ecosystem services? The need for standardized environmental accounting units. *Ecological Economics*, *63*(2), 616-626. https://doi.org/https://doi.org/10.1016/j.ecolecon.2007.01.002

Bridges, T. S., Burks-Copes, K. A., Bates, M. E., Collier, Z. A., Fischenich, J. C., Piercy, C. D., Russo, E. J., Shafer, D. J., Suedel, B. C., & Gailani, J. Z. (2015). *Use of natural and nature-based features (nnbf) for coastal resilience*. US Army Engineer Research and Development Center, Environmental Laboratory ….

Brinson, M. M. (1993). *A hydrogeomorphic clasification for wetlands* (WRP-DE-4). (Technical Report (Wetlants Research Program (U.S.)), Issue. U. S. A. E. W. E. Station. https://hdl.handle.net/11681/6483

Bulleri, F., & Chapman, M. G. (2010). The introduction of coastal infrastructure as a driver of change in marine environments. *Journal of Applied Ecology*, *47*(1), 26-35. https://doi.org/https://doi.org/10.1111/j.1365-2664.2009.01751.x

Cañizares, R., & Irish, J. L. (2008). Simulation of storm-induced barrier island morphodynamics and flooding. *Coastal Engineering*, *55*(12), 1089-1101. https://doi.org/https://doi.org/10.1016/j.coastaleng.2008.04.006

Carter, N. T. a. E. L. (2020). Flood risk reduction from natural and nature-based features: Army corps of engineers authorities. *Congressional Research Service*.

Chester, M., Underwood, B. S., Allenby, B., Garcia, M., Samaras, C., Markolf, S., Sanders, K., Preston, B., & Miller, T. R. (2021). Infrastructure resilience to navigate increasingly uncertain and complex conditions in the anthropocene. *npj Urban Sustainability*, *1*(1). https://doi.org/10.1038/s42949-021-00016-y

Cohen, D. (2019). About 60.2m live in areas most vulnerable to hurricanes. *America Counts: Stories Behind the Numbers*. https://www.census.gov/library/stories/2019/07/millions-of-americans-live-coastline-regions.html

Costanza, R., d'Arge, R., de Groot, R., Farber, S., Grasso, M., Hannon, B., Limburg, K., Naeem, S., O'Neill, R. V., Paruelo, J., Raskin, R. G., Sutton, P., & van den Belt, M. (1997). The value of the world's ecosystem services and natural capital. *Nature*, *387*(6630), 253-260. https://doi.org/10.1038/387253a0

Crosby, S. C., Sax, D. F., Palmer, M. E., Booth, H. S., Deegan, L. A., Bertness, M. D., & Leslie, H. M. (2016). Salt marsh persistence is threatened by predicted sea-level rise. *Estuarine, Coastal and Shelf Science*, *181*, 93-99. https://doi.org/10.1016/j.ecss.2016.08.018

Daily, G. C. (1997). Introduction:What are ecosystem services. In *Nature's services: Societal dependence on natural ecosystems*. Island Press.

Dietrich, J. C., Tanaka, S., Westerink, J. J., Dawson, C. N., Luettich, R. A., Zijlema, M., Holthuijsen, L. H., Smith, J. M., Westerink, L. G., & Westerink, H. J. (2012). Performance of the unstructured-mesh, swan+adcirc model in computing hurricane waves and surge. *Journal of Scientific Computing*, *52*(2), 468-497. https://doi.org/10.1007/s10915-011-9555-6

Dietrich, J. C., Zijlema, M., Westerink, J. J., Holthuijsen, L. H., Dawson, C., Luettich, R. A., Jensen, R. E., Smith, J. M., Stelling, G. S., & Stone, G. W. (2011). Modeling hurricane waves and storm surge using integrally-coupled, scalable computations. *Coastal Engineering*, *58*(1), 45-65. https://doi.org/10.1016/j.coastaleng.2010.08.001

Doran, K. S., Long, J.W., Birchler, J.J., Brenner, O.T., Hardy, M.W., Morgan, K.L.M, Stockdon, H.F., and Torres, M.L. (2017). *Lidar-derived beach morphology (dune crest, dune toe, and shoreline) for u.S. Sandy coastlines (ver. 4.0, october 2020* https://doi.org/https://doi.org/10.5066/F7GF0S0Z

Elizabeth Murray, J. C., Lisa Wainger, David J. Tazik. (2013). *Incorporating ecosystem good and services in environmental planning - definitions, classification and operational approaches* (TN-EMRRP-ER-18). U. S. A. C. o. Engineers.

Fisher, B., Turner, R. K., & Morling, P. (2009). Defining and classifying ecosystem services for decision making. *Ecological Economics*, *68*(3), 643-653. https://doi.org/https://doi.org/10.1016/j.ecolecon.2008.09.014

Galland, J.-C., Goutal, N., & Hervouet, J.-M. (1991). Telemac: A new numerical model for solving shallow water equations. *Advances in water resources*, *14*(3), 138-148.

Gedan, K. B., Kirwan, M. L., Wolanski, E., Barbier, E. B., & Silliman, B. R. (2011). The present and future role of coastal wetland vegetation in protecting shorelines: Answering recent challenges to the paradigm. *Climatic Change*, *106*(1), 7-29. https://doi.org/10.1007/s10584-010-0003-7

Gersonius, B., Ashley, R., Pathirana, A., & Zevenbergen, C. (2013). Climate change uncertainty: Building flexibility into water and flood risk infrastructure. *Climatic Change*, *116*(2), 411-423. https://doi.org/10.1007/s10584-012-0494-5

Glass, E. M., Garzon, J. L., Lawler, S., Paquier, E., & Ferreira, C. M. (2018). Potential of marshes to attenuate storm surge water level in the chesapeake bay. *Limnology and Oceanography*, *63*(2), 951-967. https://doi.org/10.1002/lno.10682

Grzegorzewski, A. S., Cialone, M. A., & Wamsley, T. V. (2011). Interaction of barrier islands and storms: Implications for flood risk reduction in louisiana and mississippi. *Journal of Coastal Research*(59), 156-164. https://doi.org/10.2112/si59-016.1

Hagen, S. C., Zundel, A. K., & Kojima, S. (2006). Automatic, unstructured mesh generation for tidal calculations in a large domain. *International Journal of Computational Fluid Dynamics*, *20*(8), 593-608. https://doi.org/10.1080/10618560601046846

Hinkel, J., Lincke, D., Vafeidis, A. T., Perrette, M., Nicholls, R. J., Tol, R. S. J., Marzeion, B., Fettweis, X., Ionescu, C., & Levermann, A. (2014). Coastal flood damage and adaptation costs under 21st century sea-level rise. *Proceedings of the National Academy of Sciences*, *111*(9), 3292-3297. https://doi.org/10.1073/pnas.1222469111

Houser, C., Hapke, C., & Hamilton, S. (2008). Controls on coastal dune morphology, shoreline erosion and barrier island response to extreme storms. *Geomorphology*, *100*(3), 223-240. https://doi.org/https://doi.org/10.1016/j.geomorph.2007.12.007

IPCC. (2021). *Climate change 2021: The physical science basis. Contribution of working group i to the sixth assessment report of the intergovernmental panel on climate change* (Vol. In Press). Cambridge University Press. https://doi.org/10.1017/9781009157896

Kim, Y., Chester, M. V., Eisenberg, D. A., & Redman, C. L. (2019). The infrastructure trolley problem [Article]. *Positioning Safe-to-fail Infrastructure for Climate Change Adaptation*, *7*(7), 704-717. https://doi.org/10.1029/2019EF001208

Koch, E. W., Barbier, E. B., Silliman, B. R., Reed, D. J., Perillo, G. M., Hacker, S. D., Granek, E. F., Primavera, J. H., Muthiga, N., Polasky, S., Halpern, B. S., Kennedy, C. J., Kappel, C. V., & Wolanski, E. (2009). Non-linearity in ecosystem services: Temporal and spatial variability in coastal protection. *Frontiers in Ecology and the Environment*, *7*(1), 29-37. https://doi.org/10.1890/080126

Kratzmann, M. G., & Hapke, C. J. (2010). Quantifying anthropogenically driven morphologic changes on a barrier island: Fire island national seashore, new york. *Journal of Coastal Research*, *28*(1), 76-88. https://doi.org/10.2112/jcoastres-d-10-00012.1

Lagarias, J. C., Reeds, J. A., Wright, M. H., & Wright, P. E. (1998). Convergence properties of the nelder--mead simplex method in low dimensions. *SIAM Journal on Optimization*, *9*(1), 112-147. https://doi.org/10.1137/s1052623496303470

Lawler, S., Haddad, J., & Ferreira, C. M. (2016). Sensitivity considerations and the impact of spatial scaling for storm surge modeling in wetlands of the mid-atlantic region. *Ocean & Coastal Management*, *134*, 226-238. https://doi.org/10.1016/j.ocecoaman.2016.10.008

Liao, K.-H. (2012). A theory on urban resilience to floods—a basis for alternative planning practices. *Ecology and Society*, *17*(4). http://www.jstor.org/stable/26269244

Loder, N. M., Irish, J. L., Cialone, M. A., & Wamsley, T. V. (2009). Sensitivity of hurricane surge to morphological parameters of coastal wetlands. *Estuarine, Coastal and Shelf Science*, *84*(4), 625-636. https://doi.org/10.1016/j.ecss.2009.07.036

Lowe, R. J., Falter, J. L., Monismith, S. G., & Atkinson, M. J. (2009). Wave-driven circulation of a coastal reef–lagoon system. *Journal of Physical Oceanography*, *39*(4), 873-893. https://doi.org/10.1175/2008jpo3958.1

Lowe, R. J., Hart, C., & Pattiaratchi, C. B. (2010). Morphological constraints to wave-driven circulation in coastal reef-lagoon systems: A numerical study. *Journal of Geophysical Research: Oceans*, *115*(C9). https://doi.org/https://doi.org/10.1029/2009JC005753

Lu, Y., Shi, F., Kobayashi, N., Malej, M., Zhu, T., & Feng, W. (2018). Numerical investigation of excessive surge induced by wave overtopping in an inlet-bay system. *Coastal Engineering*, *140*, 383-394. https://doi.org/https://doi.org/10.1016/j.coastaleng.2018.08.009

Luettich, R. A. W., Joannes J. (2004). Formulation and numerical implementation of the 2d/3d adcirc finite element model version 44.Xx.

Luettich, R. A. W., Joannes J.; Scheffner, Norman W. (1992). Adcirc: An advanced three-dimensional circulation model for shelves, coasts, and estuaries. Report 1, theory and methodology of adcirc-2dd1 and adcirc-3dl [Technical Report]. https://hdl.handle.net/11681/4618

M.E.A. (2005). Ecosystems and human well-being: Synthesis. In *Millenium ecosystem assessment*. Island Press.

Magliocca, N. R., McNamara, D. E., & Murray, A. B. (2011). Long-term, large-scale morphodynamic effects of artificial dune construction along a barrier island coastline. *Journal of Coastal Research*, *27*(5), 918-930. https://doi.org/10.2112/jcoastres-d-10-00088.1

Masselink, G., & van Heteren, S. (2014). Response of wave-dominated and mixed-energy barriers to storms. *Marine Geology*, *352*, 321-347. https://doi.org/https://doi.org/10.1016/j.margeo.2013.11.004

McCabe, G. J., Clark, M. P., & Serreze, M. C. (2001). Trends in northern hemisphere surface cyclone frequency and intensity. *Journal of Climate*, *14*(12), 2763-2768. https://doi.org/10.1175/1520-0442(2001)014<2763:Tinhsc>2.0.Co;2

McCall, R. T., Van Thiel de Vries, J. S. M., Plant, N. G., Van Dongeren, A. R., Roelvink, J. A., Thompson, D. M., & Reniers, A. J. H. M. (2010). Two-dimensional time dependent hurricane overwash and erosion modeling at santa rosa island. *Coastal Engineering*, *57*(7), 668-683. https://doi.org/https://doi.org/10.1016/j.coastaleng.2010.02.006

Medlin, S. D., & Bilskie, M. V. (2022). *Barrier_island_morphology_database*. https://github.com/uga-coast/Barrier_Island_Morphology_Database

Medlin, S. D., Hewageegana, V. H., & Bilskie, M. V. (2022). *Barrier_island_landscape_generator*. https://github.com/uga-coast/Barrier_Island_LandScape_Generator

Medlin, S. D., Santiago-Collazo, F. L., & Bilskie, M. V. (2022). *Adcirc_utilities*. https://github.com/uga-coast/ADCIRC_Utilities

Miselis, J. L., & Lorenzo-Trueba, J. (2017). Natural and human-induced variability in barrier-island response to sea level rise. *Geophysical Research Letters*, *44*(23), 11,922-911,931. https://doi.org/https://doi.org/10.1002/2017GL074811

Morris, R. L., Konlechner, T. M., Ghisalberti, M., & Stephen. (2018). From grey to green: Efficacy of eco-engineering solutions for nature-based coastal defence. *Global Change Biology*, *24*(5), 1827-1842. https://doi.org/10.1111/gcb.14063

Mulhern, J. S., Johnson, C. L., & Martin, J. M. (2017). Is barrier island morphology a function of tidal and wave regime? *Marine Geology*, *387*, 74-84. https://doi.org/https://doi.org/10.1016/j.margeo.2017.02.016

Murshid, S., & Mariotti, G. (2021). Geometry of natural and engineered tidal inlets. *Coastal Engineering*, *164*, 103828. https://doi.org/https://doi.org/10.1016/j.coastaleng.2020.103828

Narayan, S., Beck, M. W., Reguero, B. G., Losada, I. J., Van Wesenbeeck, B., Pontee, N., Sanchirico, J. N., Ingram, J. C., Lange, G.-M., & Burks-Copes, K. A. (2016). The effectiveness, costs and coastal protection benefits of natural and nature-based defences. *PLOS ONE*, *11*(5), e0154735. https://doi.org/10.1371/journal.pone.0154735

NCEI. (2022). *U.S. Billion-dollar weather and climate disasters*. Retrieved from https://www.ncei.noaa.gov/access/billions/

Needham, H. F., & Keim, B. D. (2012). A storm surge database for the us gulf coast. *International Journal of Climatology*, *32*(14), 2108-2123. https://doi.org/10.1002/joc.2425

Network for engineering with nature. (2022). Retrieved June 5, 2022 from https://n-ewn.org/

NOAA. (2015). *Guidance for considering the use of living shorelines*.

Oliver, B., & Ramirez-Avila, J. J. (2019). Barrier island restoration: A literature review. In *World environmental and water resources congress 2019* (pp. 310-319). https://doi.org/doi:10.1061/9780784482353.029

Passeri, D. L., Bilskie, M. V., Hagen, S. C., Mickey, R. C., Dalyander, P. S., & Gonzalez, V. M. (2021). Assessing the effectiveness of nourishment in decadal barrier island morphological resilience. *Water*, *13*(7), 944. https://doi.org/10.3390/w13070944

Passeri, D. L., Bilskie, M. V., Plant, N. G., Long, J. W., & Hagen, S. C. (2018). Dynamic modeling of barrier island response to hurricane storm surge under future sea level rise. *Climatic Change*, *149*(3), 413-425. https://doi.org/10.1007/s10584-018-2245-8

Passeri, D. L., Dalyander, P. S., Long, J. W., Mickey, R. C., Jenkins III, R. L., Thompson, D. M., Plant, N. G., Godsey, E. S., & Gonzalez, V. M. (2020). The roles of storminess and sea level rise in decadal barrier island evolution. *Geophysical Research Letters*, *47*(18), e2020GL089370. https://doi.org/10.1029/2020gl089370

Peter Kareiva, H. T., Taylor H. Ricketts, Gretchen C. Daily, and Stephen Polasky. (2011). *Natural capital theory & practice of mapping ecosystem services* (H. T. Peter Kareiva, Taylor H. Ricketts, Gretchen C. Daily, and Stephen Polasky, Ed.). Oxford University Press.

Rego, J. L., & Li, C. (2010). Storm surge propagation in galveston bay during hurricane ike. *Journal of Marine Systems*, *82*(4), 265-279. https://doi.org/https://doi.org/10.1016/j.jmarsys.2010.06.001

Roelvink, D., Reniers, A., Van Dongeren, A., Van Thiel De Vries, J., McCall, R., & Lescinski, J. (2009). Modelling storm impacts on beaches, dunes and barrier islands. *Coastal Engineering*, *56*(11-12), 1133-1152. https://doi.org/10.1016/j.coastaleng.2009.08.006

Roelvink, J. A., & Van Banning, G. K. F. M. (1995). Design and development of delft3d and application to coastal morphodynamics. *Oceanographic Literature Review*, *42*(11), 925.

Rogers, L. J., Moore, L. J., Goldstein, E. B., Hein, C. J., Lorenzo-Trueba, J., & Ashton, A. D. (2015). Anthropogenic controls on overwash deposition: Evidence and consequences. *Journal of Geophysical Research: Earth Surface*, *120*(12), 2609-2624. https://doi.org/https://doi.org/10.1002/2015JF003634

Rosati, J. (2009). *Barrier island migration over a consolidating substrate*

Rosati, J., Stone, G., Dean, R., & Kraus, N. (2006). Restoration of barrier islands overlying poorly-consolidated sediments, south-central louisiana. *Gulf Coast Association of Geological Societies Transactions*, *56*.

Rosati, J. D., Touzinsky, K. F., & Lillycrop, W. J. (2015). Quantifying coastal system resilience for the us army corps of engineers. *Environment Systems and Decisions*, *35*(2), 196-208. https://doi.org/10.1007/s10669-015-9548-3

Saleh, F., & Weinstein, M. P. (2016). The role of nature-based infrastructure (nbi) in coastal resiliency planning: A literature review. *Journal of Environmental Management*, *183*, 1088-1098. https://doi.org/10.1016/j.jenvman.2016.09.077

Schuerch, M., Spencer, T., Temmerman, S., Kirwan, M. L., Wolff, C., Lincke, D., McOwen, C. J., Pickering, M. D., Reef, R., Vafeidis, A. T., Hinkel, J., Nicholls, R. J., & Brown, S. (2018). Future response of global coastal wetlands to sea-level rise. *Nature*, *561*(7722), 231-234. https://doi.org/10.1038/s41586-018-0476-5

Schultz, M. T., McKay, S. Kyle, Hales, Lyndell Z. (2012). The quantification and evolution of resilience in integrated coastal systems [Technical Report]. *ERDC TR*, Article 12-7.

Smith, C., Nicholls, Z. R. J., Armour, K., Collins, W., Forster, P., Meinshausen, M., Palmer, M. D., & Watanabe, M. (2021). The earth's energy budget, climate feedbacks, and climate sensitivity supplementary material. In V. Masson-Delmotte, P. Zhai, A. Pirani, S. L. Connors, C. Péan, S. Berger, N. Caud, Y. Chen, L. Goldfarb, M. I. Gomis, M. Huang, K. Leitzell, E. Lonnoy, J. B. R. Matthews, T. K. Maycock, T. Waterfield, O. Yelekçi, R. Yu,

& B. Zhou (Eds.), *Climate change 2021: The physical science basis. Contribution of working group i to the sixth assessment report of the intergovernmental panel on climate change*. Available from https://www.ipcc.ch/

Smolders, S., João Teles, M., Leroy, A., Maximova, T., Meire, P., & Temmerman, S. (2020). Modeling storm surge attenuation by an integrated nature-based and engineered flood defense system in the scheldt estuary (belgium). *Journal of Marine Science and Engineering*, *8*(1), 27. https://doi.org/10.3390/jmse8010027

Suhayda, J. N. (1997). Modeling impacts of louisiana barrier islands on wetland hydroogy. *Journal of Coastal Research*, *13*(3), 686-693. https://doi.org/10.2307/4298664

Sutton-Grier, A., Gittman, R., Arkema, K., Bennett, R., Benoit, J., Blitch, S., Burks-Copes, K., Colden, A., Dausman, A., Deangelis, B., Hughes, A., Scyphers, S., & Grabowski, J. (2018). Investing in natural and nature-based infrastructure: Building better along our coasts. *Sustainability*, *10*(2), 523. https://doi.org/10.3390/su10020523

Terry Dinan, D. W. (2019). *Expected costs of damage from hurricane winds and storm-related flooding*. (55019). Congress of the United States

USACE. (2017). *Nationwide permit (54) living shorelines*.

Villaret, C., Hervouet, J.-M., Kopmann, R., Merkel, U., & Davies, A. G. (2013). Morphodynamic modeling using the telemac finite-element system. *Computers & Geosciences*, *53*, 105-113. https://doi.org/https://doi.org/10.1016/j.cageo.2011.10.004

Wamsley, T., Cialone, M., Smith, J., Atkinson, J., & Rosati, J. (2010). The potential of wetlands in reducing storm surge. *Ocean Engineering*, *37*, 59-68. https://doi.org/10.1016/j.oceaneng.2009.07.018

Wamsley, T. V., Cialone, M. A., Smith, J. M., Ebersole, B. A., & Grzegorzewski, A. S. (2009). Influence of landscape restoration and degradation on storm surge and waves in southern louisiana. *Natural Hazards*, *51*(1), 207-224. https://doi.org/10.1007/s11069-009-9378-z

Westerink, J., Luettich, J. R., Blain, C., & Scheffner, N. (1994). Adcirc: An advanced three-dimensional circulation model for shelves, coasts, and estuaries. Report 2. User's manual for adcirc-2ddi. 168.

Westerink, J. J., Luettich, R. A., Feyen, J. C., Atkinson, J. H., Dawson, C., Roberts, H. J., Powell, M. D., Dunion, J. P., Kubatko, E. J., & Pourtaheri, H. (2008). A basin- to channel-scale unstructured grid hurricane storm surge model applied to southern louisiana. *Monthly Weather Review*, *136*(3), 833-864. https://doi.org/10.1175/2007mwr1946.1

Wood, M., Kovacs, D., Bostrom, A., Bridges, T., & Linkov, I. (2012). Flood risk management: Us army corps of engineers and layperson perceptions. *Risk Analysis*, *32*(8), 1349-1368. https://doi.org/10.1111/j.1539-6924.2012.01832.x

Zhang, K., Liu, H., Li, Y., Xu, H., Shen, J., Rhome, J., & Smith, T. J. (2012). The role of mangroves in attenuating storm surges. *Estuarine, Coastal and Shelf Science*, *102-103*, 11-23. https://doi.org/10.1016/j.ecss.2012.02.021

APPENDIX A DISTRIBUTIONS OF BARRIER ISLAND PARAMETERS

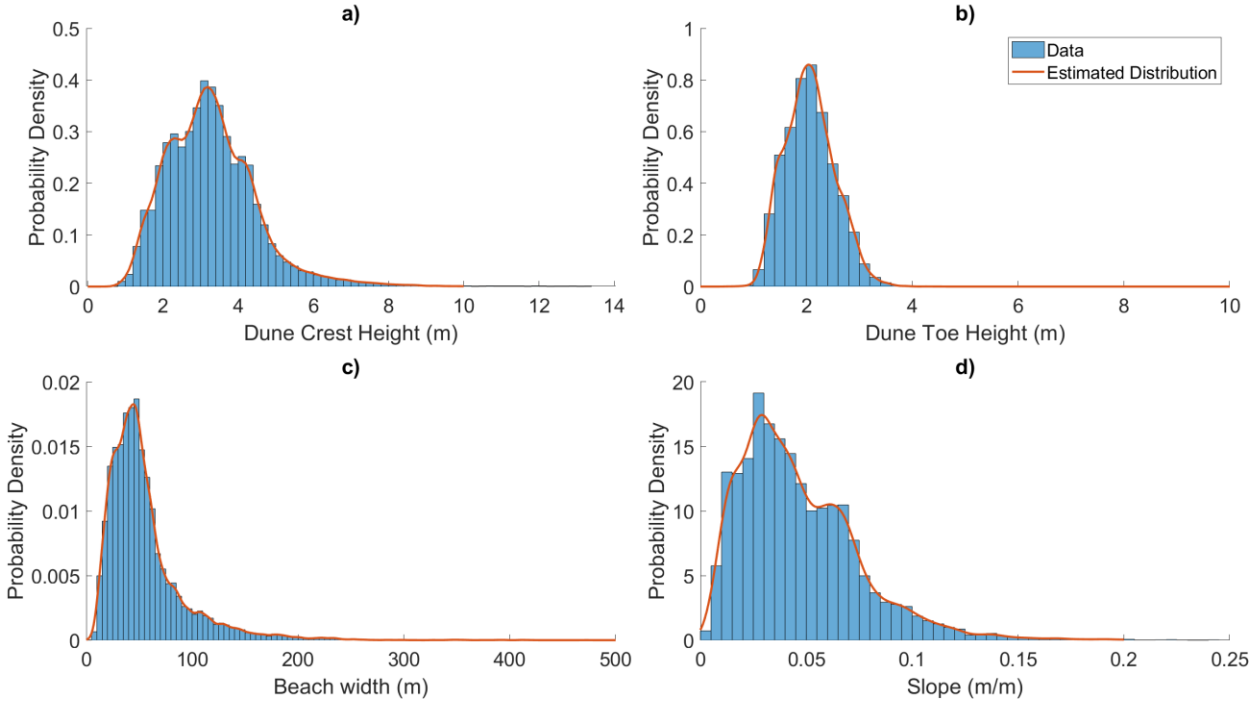

Figure A.1: Histograms and normal Kernel density estimations of a) Dune Crest Height, b) Dune Toe Height, c) Beach Width, d) Beach Slope for observed data. Kernel density estimates were used as all data failed the K-S test for the standard normal distribution at the 5% significance level.

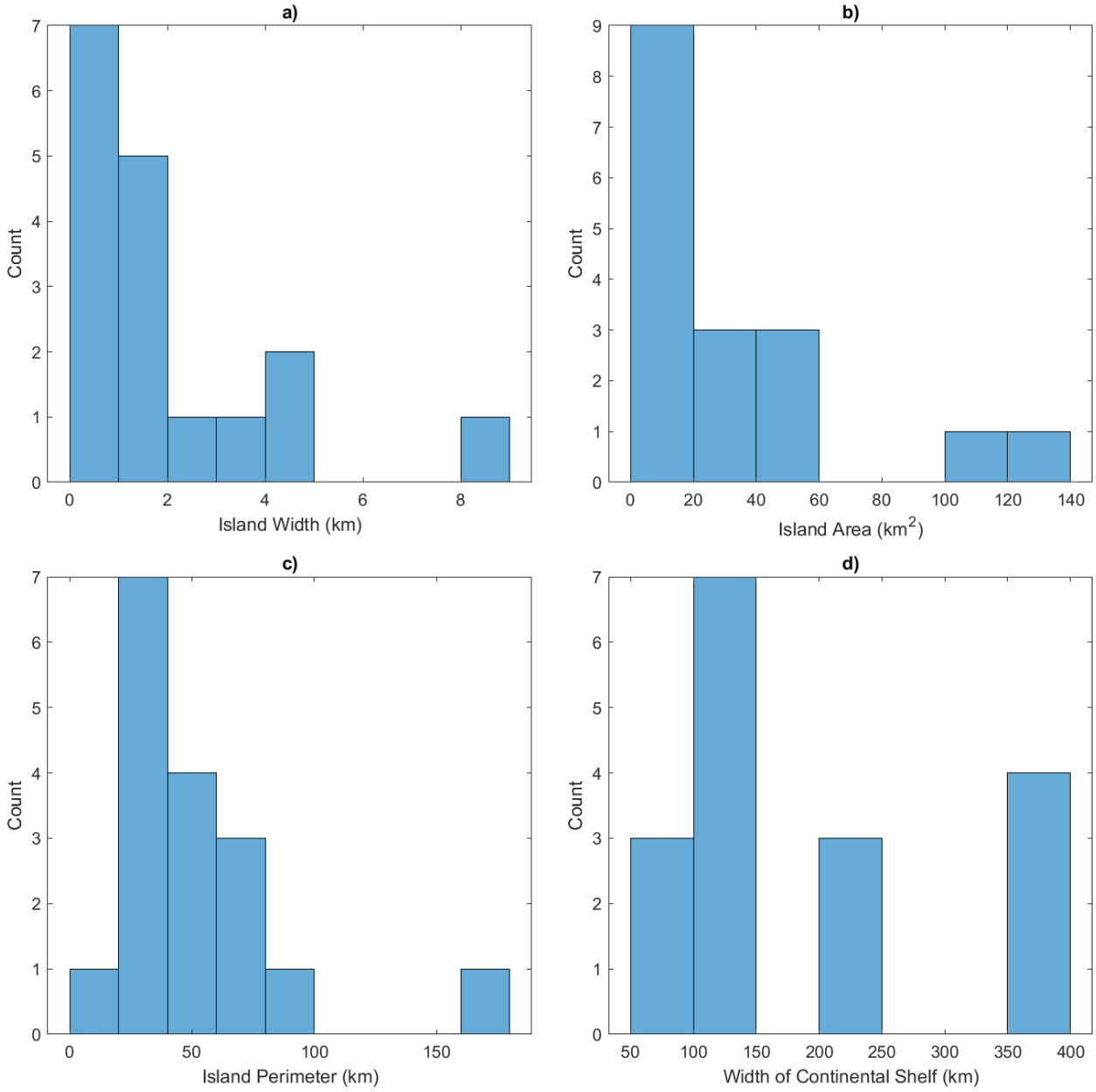

Figure A.2: Histograms of a) Island Width, b) Island Area, c) Island Perimeter, d) Width of the Continental Shelf, d) Depth of Closure

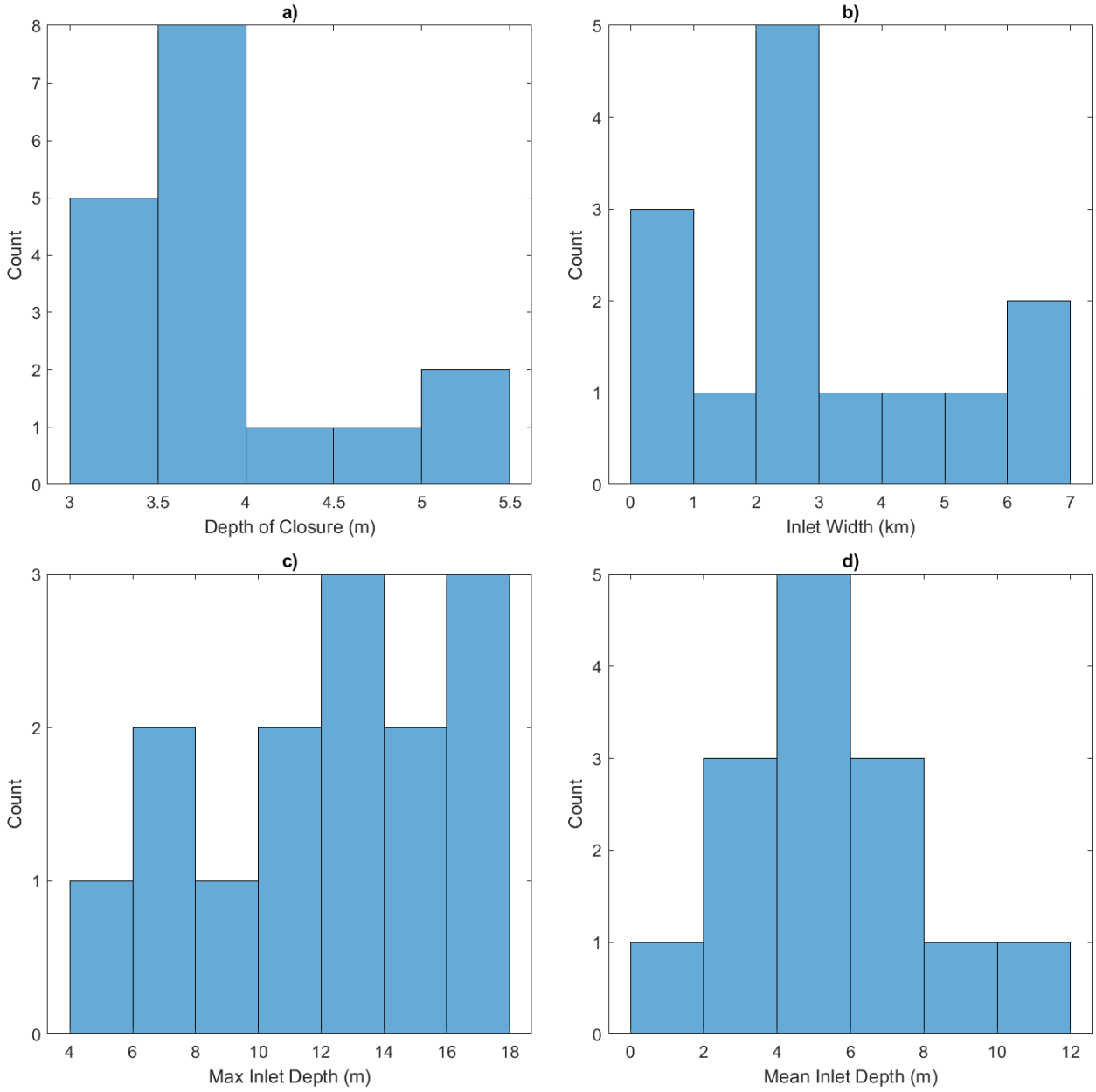

Figure A.3: Histograms of a) Depth of Closure, b) Minimum Inlet Width, c) Maximum Inlet Depth, and d) Mean Inlet Depth

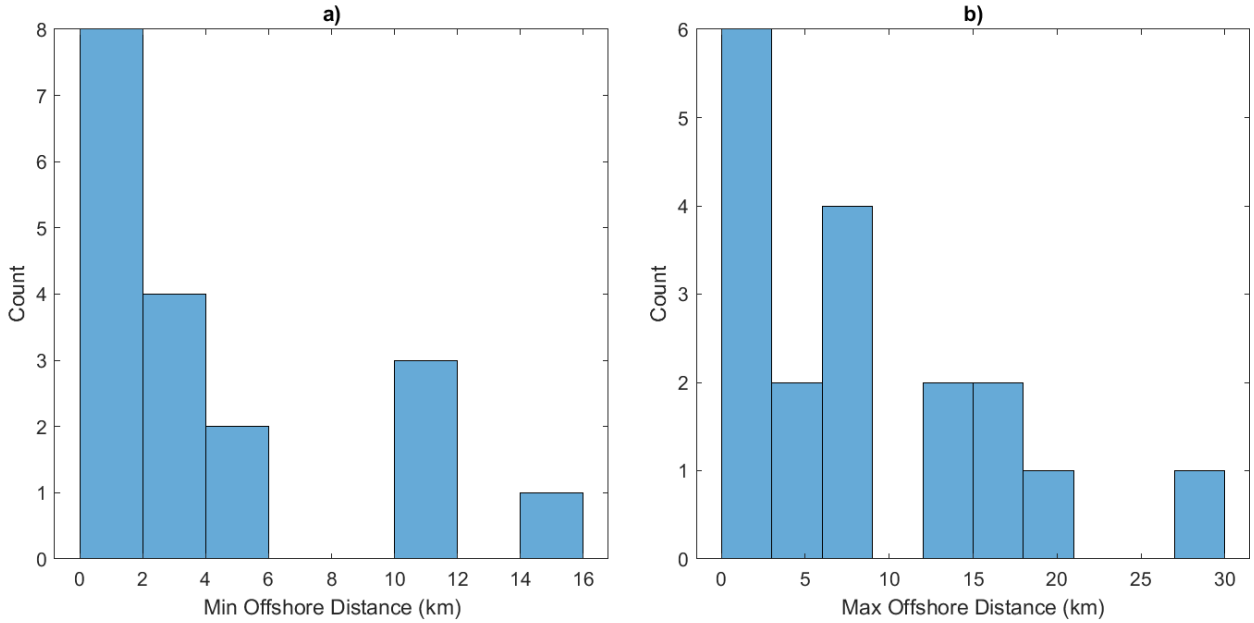

Figure A.4: Histograms for a) Minimum Distance between BI and the mainland and b) Maximum distance between BI and the mainland

.

APPENDIX B INLET RATIO VS MAX SURGE ATTENUATION

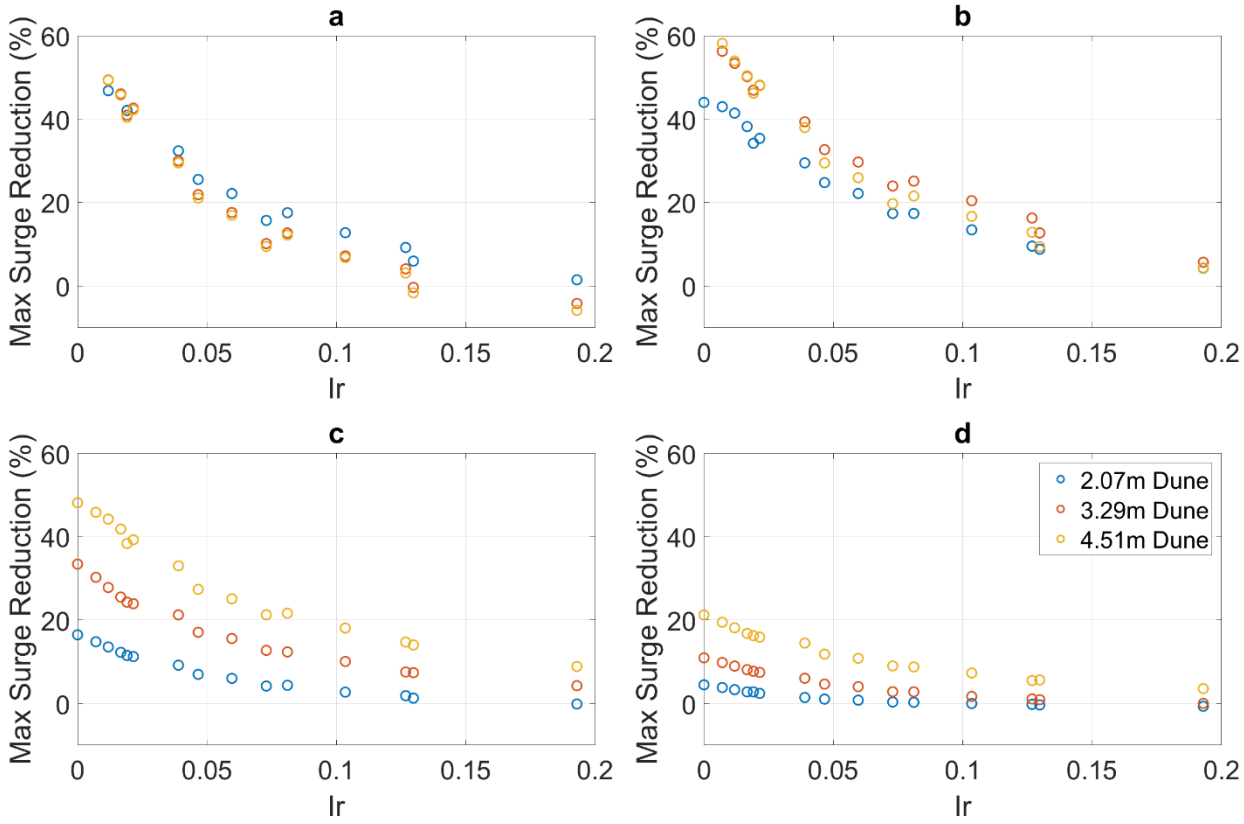

Figure B.1: Effect of Inlet Ratio on maximum water levels for various peak dune heights and storm surge with an 8-hour duration and a) 1m amplitude b) 2m amplitude c) 4m amplitude c) 6m amplitude.

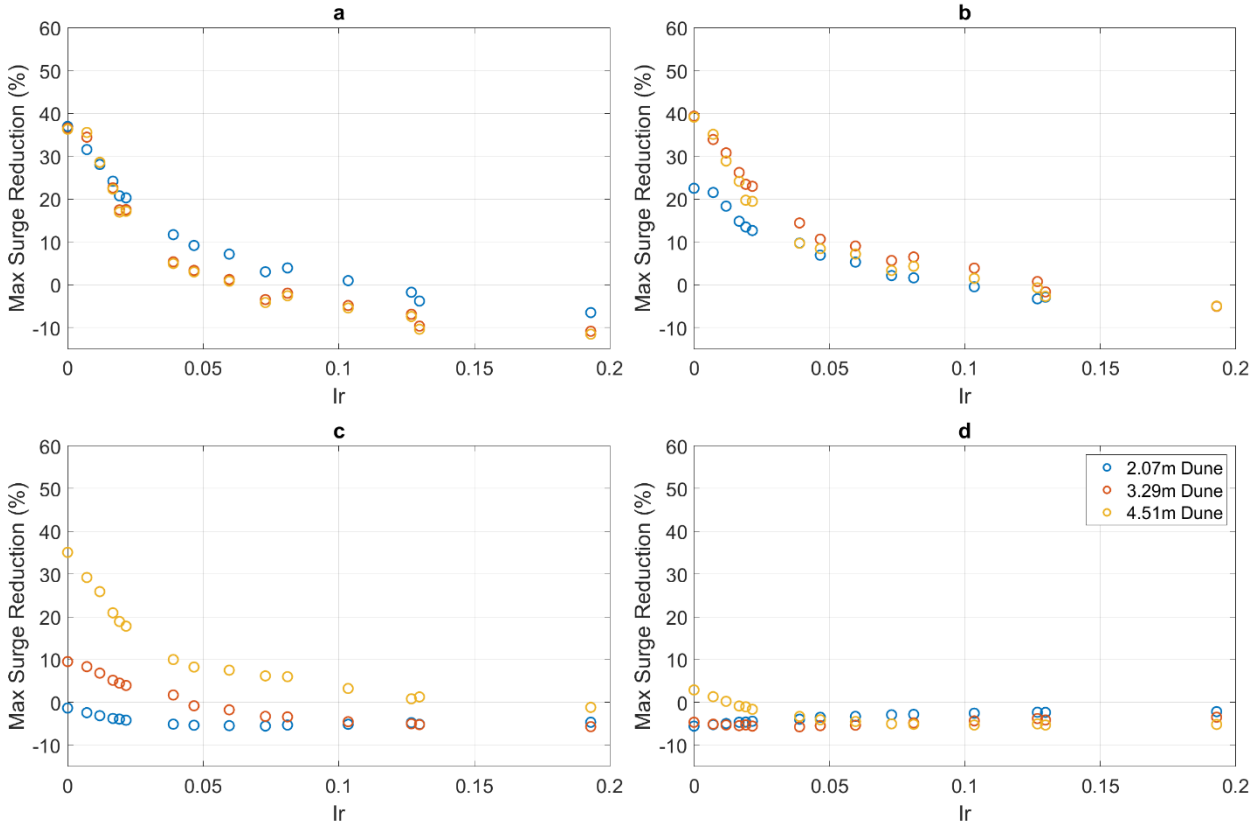

Figure B.2: Effect of Inlet Ratio on maximum water levels for various peak dune heights and storm surge with a 12-hour duration and a) 1m amplitude b) 2m amplitude c) 4m amplitude c) 6m amplitude.

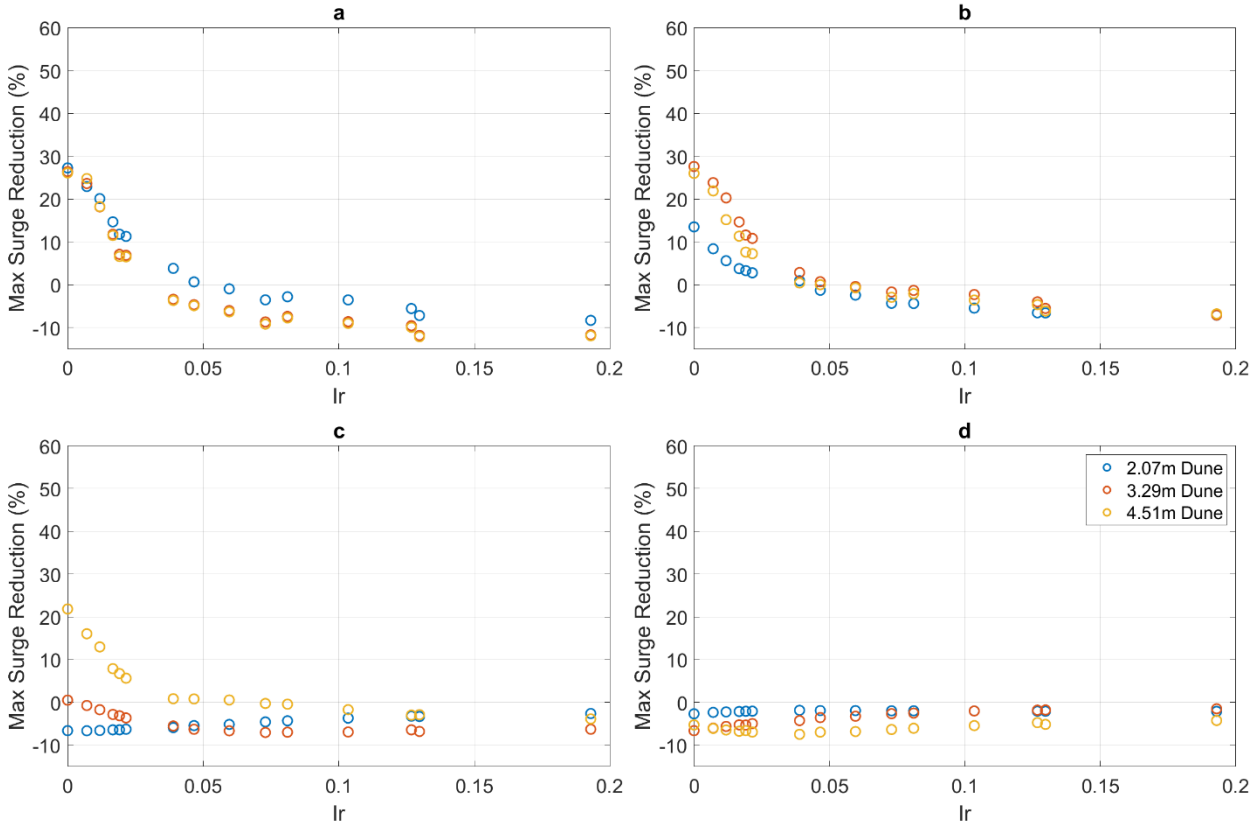

Figure B.3: Effect of Inlet Ratio on maximum water levels for various peak dune heights and storm surge with a 24-hour duration and a) 1m amplitude b) 2m amplitude c) 4m amplitude c) 6m amplitude.

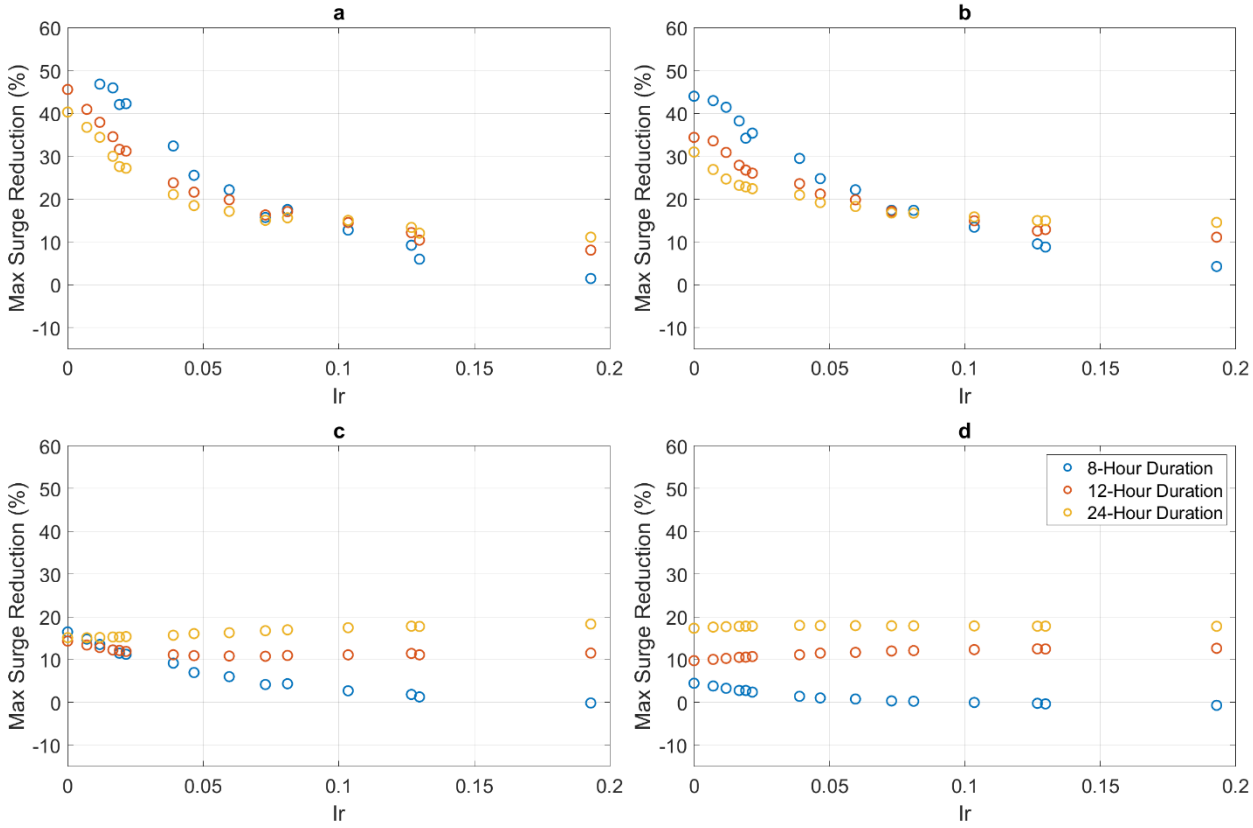

Figure B.4: Inlet Ratio vs maximum water levels for a 2.07m dune over various storm surge durations and surges with a) 1m amplitude, b) 2m amplitude, c) 4m amplitude, and d) 6m amplitude.

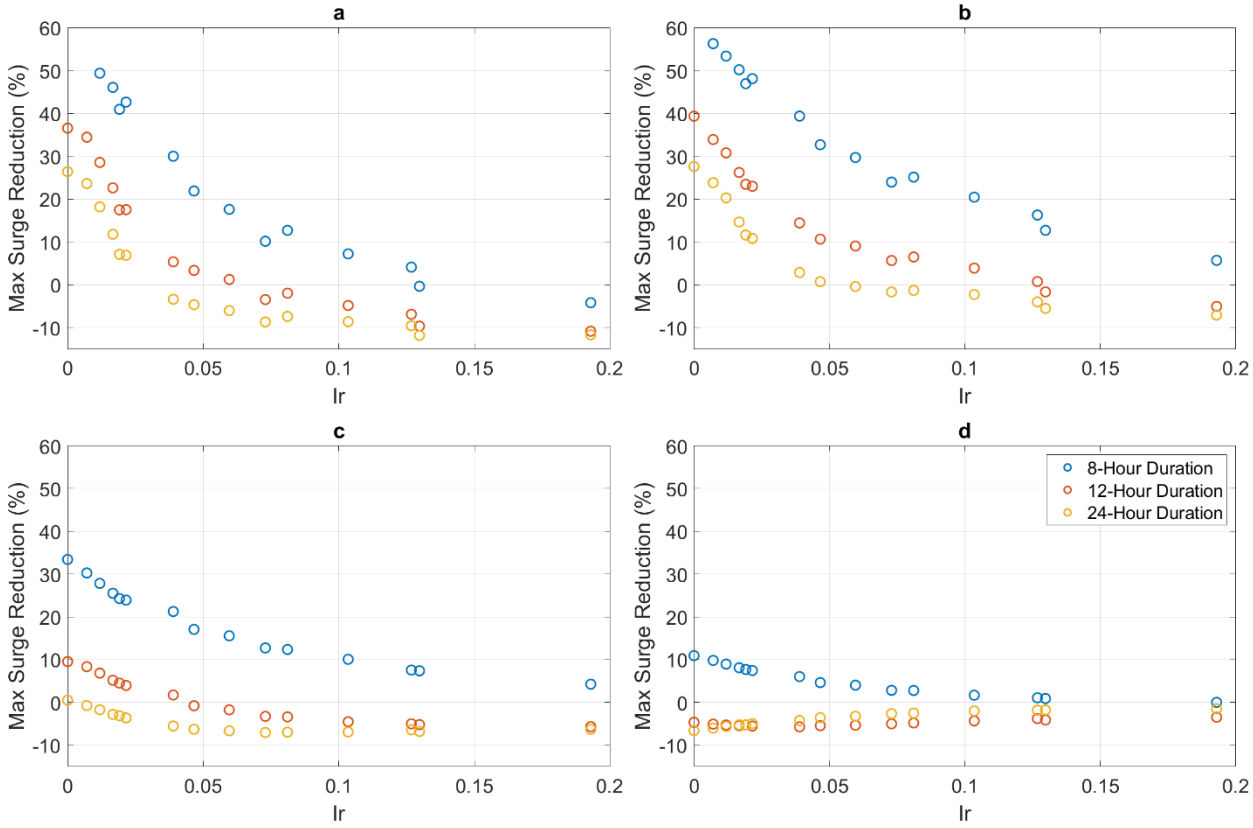

Figure B.5: Inlet Ratio vs maximum water levels for a 3.29m dune over various storm surge durations and surges with a) 1m amplitude, b) 2m amplitude, c) 4m amplitude, and d) 6m amplitude.

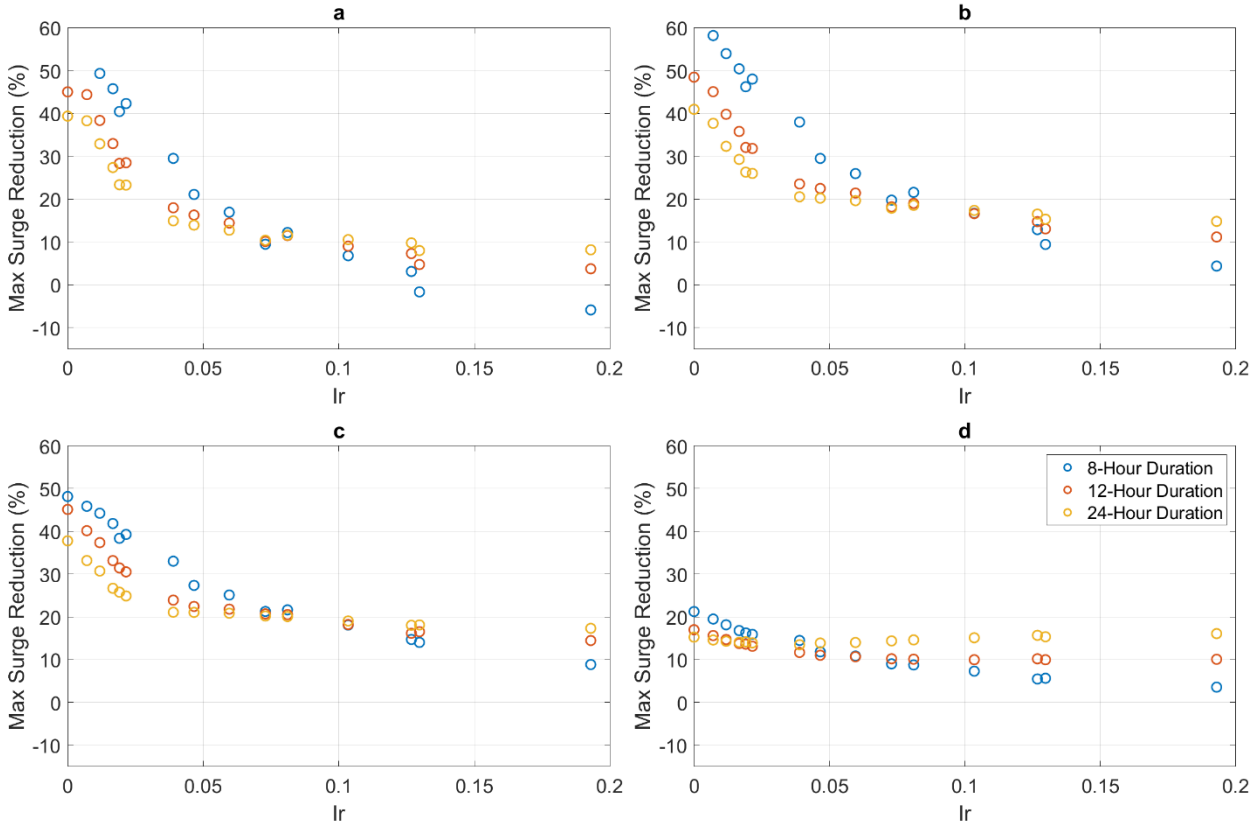

Figure B.6; Inlet Ratio vs maximum water levels for a 4.51m dune over various storm surge durations and surges with a) 1m amplitude, b) 2m amplitude, c) 4m amplitude, and d) 6m amplitude.